



## A novel *N*-heterocycles substituted oseltamivir derivatives as potent inhibitors of influenza virus neuraminidase: discovery, synthesis and biological evaluation

Jiwei Zhang, Chuanfeng Liu, Ruifang Jia, Xujie Zhang, Jian Zhang, Chiara Bertagnin, Anna Bonomini, Laura Guizzo, Yuanmin Jiang, Huinan Jia, Shuzhen Jia, Xiuli Ma, Arianna Loregian, Bing Huang, Peng Zhan & Xinyong Liu

**To cite this article:** Jiwei Zhang, Chuanfeng Liu, Ruifang Jia, Xujie Zhang, Jian Zhang, Chiara Bertagnin, Anna Bonomini, Laura Guizzo, Yuanmin Jiang, Huinan Jia, Shuzhen Jia, Xiuli Ma, Arianna Loregian, Bing Huang, Peng Zhan & Xinyong Liu (2023) A novel *N*-heterocycles substituted oseltamivir derivatives as potent inhibitors of influenza virus neuraminidase: discovery, synthesis and biological evaluation, *Journal of Enzyme Inhibition and Medicinal Chemistry*, 38:1, 2277135, DOI: [10.1080/14756366.2023.2277135](https://doi.org/10.1080/14756366.2023.2277135)

**To link to this article:** <https://doi.org/10.1080/14756366.2023.2277135>



© 2023 The Author(s). Published by Informa UK Limited, trading as Taylor & Francis Group.



[View supplementary material](#)



Published online: 13 Nov 2023.



[Submit your article to this journal](#)



Article views: 1046



[View related articles](#)



[View Crossmark data](#)

RESEARCH ARTICLE



## A novel N-heterocycles substituted oseltamivir derivatives as potent inhibitors of influenza virus neuraminidase: discovery, synthesis and biological evaluation

Jiwei Zhang<sup>a\*</sup>, Chuanfeng Liu<sup>a,b\*</sup>, Ruifang Jia<sup>a</sup>, Xujie Zhang<sup>a</sup>, Jian Zhang<sup>c</sup>, Chiara Bertagnin<sup>d</sup>, Anna Bonomini<sup>d</sup>, Laura Guizzo<sup>d</sup>, Yuanmin Jiang<sup>a</sup>, Huinan Jia<sup>a</sup>, Shuzhen Jia<sup>a</sup>, Xiuli Ma<sup>e</sup>, Arianna Loregian<sup>d</sup>, Bing Huang<sup>e</sup>, Peng Zhan<sup>a,f</sup> and Xinyong Liu<sup>a,f</sup>

<sup>a</sup>Department of Medicinal Chemistry, Key Laboratory of Chemical Biology (Ministry of Education), School of Pharmaceutical Sciences, Cheeloo College of Medicine, Shandong University, Jinan, Shandong, P.R. China; <sup>b</sup>Suzhou Research Institute of Shandong University, Suzhou, Jiangsu, P.R. China; <sup>c</sup>Institute of Medical Sciences, The Second Hospital, Shandong University, Jinan, Shandong, P.R. China; <sup>d</sup>Department of Molecular Medicine, University of Padova, Padova, Italy; <sup>e</sup>Institute of Poultry Science, Shandong Academy of Agricultural Sciences, Jinan, Shandong, P.R. China; <sup>f</sup>China-Belgium Collaborative Research Center for Innovative Antiviral Drugs of Shandong Province, Jinan, Shandong, PR China

### ABSTRACT

Our previous studies have shown that the introduction of structurally diverse benzyl side chains at the C5-NH<sub>2</sub> position of oseltamivir to occupy 150-cavity contributes to the binding affinity with neuraminidase and anti-influenza activity. To obtain broad-spectrum neuraminidase inhibitors, we designed and synthesised a series of novel oseltamivir derivatives bearing different N-heterocycles substituents that have been proved to induce opening of the 150-loop of group-2 neuraminidases. Among them, compound **6k** bearing 4-((*r*)-2-methylpyrrolidin-1-yl) benzyl group exhibited antiviral activities similar to or weaker than those of oseltamivir carboxylate against H1N1, H3N2, H5N1, H5N6 and H5N1-H274Y mutant neuraminidases. More encouragingly, **6k** displayed nearly 3-fold activity enhancement against H3N2 virus over oseltamivir carboxylate and 2-fold activity enhancement over zanamivir. Molecular docking studies provided insights into the explanation of its broad-spectrum potency against wild-type neuraminidases. Overall, as a promising lead compound, **6k** deserves further optimisation by fully considering the ligand induced flexibility of the 150-loop.

### ARTICLE HISTORY

Received 21 April 2023  
Revised 27 September 2023  
Accepted 6 October 2023

### KEYWORDS

Influenza virus;  
neuraminidase inhibitors;  
150-cavity; oseltamivir; drug  
design

### Introduction

Influenza virus, the “silent terrorist” of the 21st century, endangers human health and social development. Influenza, mainly caused by influenza A virus, is still one of the most grievous global epidemics, with an estimated about 3–5 million cases of severe illness and 290,000–650,000 deaths annually all over the world<sup>1,2</sup>. In the past, several influenza A (Flu A) pandemics have caused enormous effects on global human population (e.g. 1918H1N1 and 2009H7N9)<sup>3</sup>. According to the latest reports, compared with SARS-CoV-2 mono-infection, co-infection with influenza viruses was associated with higher morbidity and mortality<sup>4</sup>.


Influenza vaccines and antiviral drugs can be used to effectively prevent and treat influenza. Although the influenza vaccines are considered the most effective measure for the prophylaxis of influenza, there are many limitations because of high variability of influenza and rapid antigenic drift; hence, the influenza vaccines are only available for the current epidemic influenza virus strains<sup>5</sup>. Additionally, the influenza vaccine must be administered annually and its effectiveness is dependent on individual immunity. Thus, antiviral drugs remain an important weapon against influenza

infections. There are currently three classes of anti-influenza agents that have been approved by the FDA (Figure 1), namely polymerase acidic protein (PA) endonuclease inhibitor (baloxavir marboxil)<sup>6</sup>, M2 ion-channel blockers (amantadine and rimantadine) and neuraminidase inhibitors (NAIs, oseltamivir, zanamivir, peramivir, and laninamivir octanoate)<sup>7–10</sup>. However, some of these licenced drugs have several drawbacks<sup>11</sup>.

Neuraminidase (NA), a crucial surface antigenic glycoprotein, is responsible for viral penetration through mucosal secretions, helping the virus to access the target cells by mucus degradation. Moreover, NA allows the detachment of the virion from infected cells and avoids the self-aggregation of progeny virions at late stages of infection by disrupting haemagglutinin–sialic acid interactions, thus promoting the release and spread of influenza virus. Among NAIs, oseltamivir phosphate, with high efficiency, high bio-availability and low toxicity, can be administered orally. However, several NA variants acquired resistance to oseltamivir, such as H274Y mutant and I117T mutant, which have seriously limited its application<sup>12,13</sup>. Consequently, there is a pressing need to develop novel improved NAIs.

**CONTACT** Bing Huang  [hbnd@163.com](mailto:hbnd@163.com)  Institute of Poultry Science, Shandong Academy of Agricultural Sciences, No. 23788 Gongye North Road, Licheng District, Jinan, Shandong Province, China; Peng Zhan  [zhanpeng1982@sdu.edu.cn](mailto:zhanpeng1982@sdu.edu.cn); Xinyong Liu  [xinyongli@sdu.edu.cn](mailto:xinyongli@sdu.edu.cn)  China-Belgium Collaborative Research Center for Innovative Antiviral Drugs of Shandong Province, No. 44, Wen Hua West Road, Lixia District, Jinan, Shandong Province, China

\*These authors contributed equally to this work.

 Supplemental data for this article can be accessed [here](#).

© 2023 The Author(s). Published by Informa UK Limited, trading as Taylor & Francis Group.

This is an Open Access article distributed under the terms of the Creative Commons Attribution-NonCommercial License (<http://creativecommons.org/licenses/by-nc/4.0/>), which permits unrestricted non-commercial use, distribution, and reproduction in any medium, provided the original work is properly cited. The terms on which this article has been published allow the posting of the Accepted Manuscript in a repository by the author(s) or with their consent.

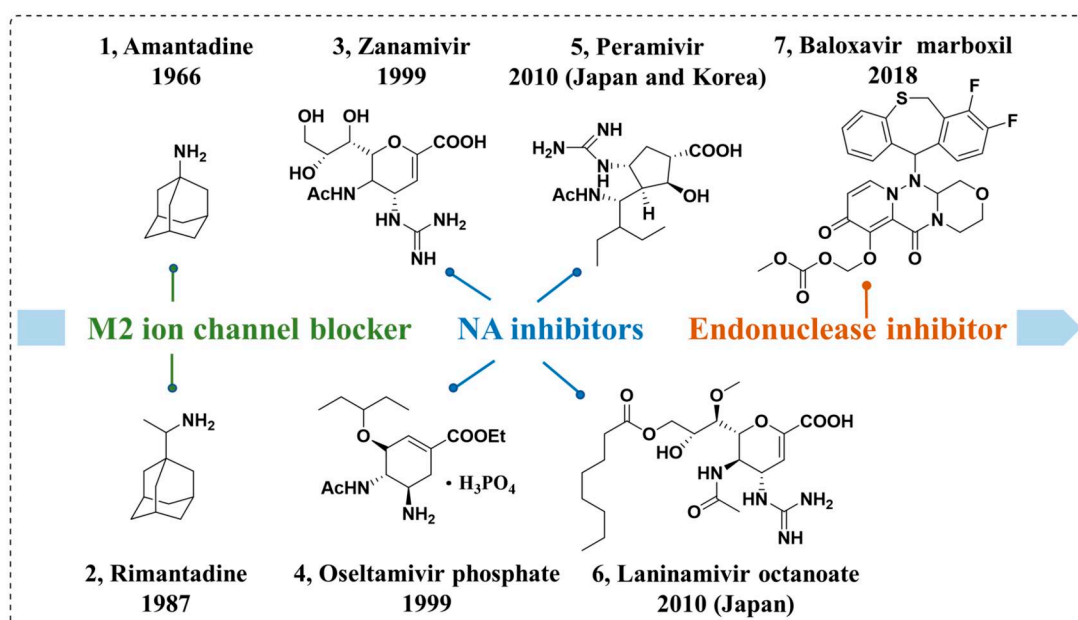


Figure 1. Structures of approved agents for the treatment of influenza viral infection.

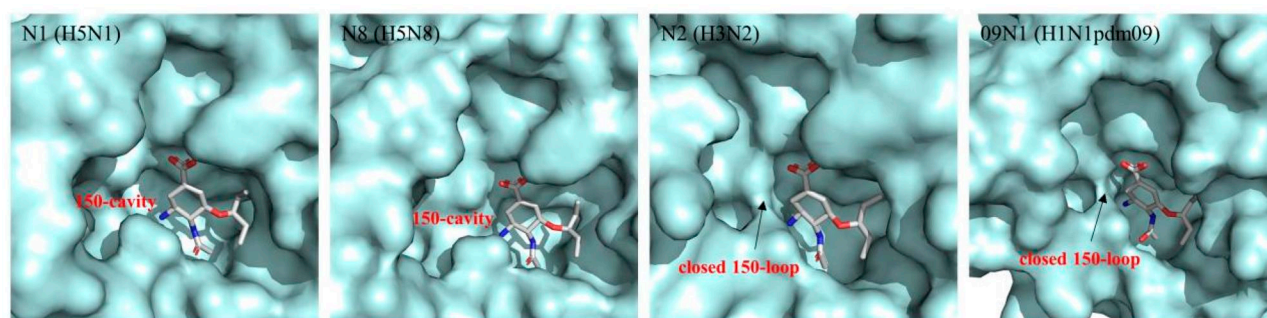


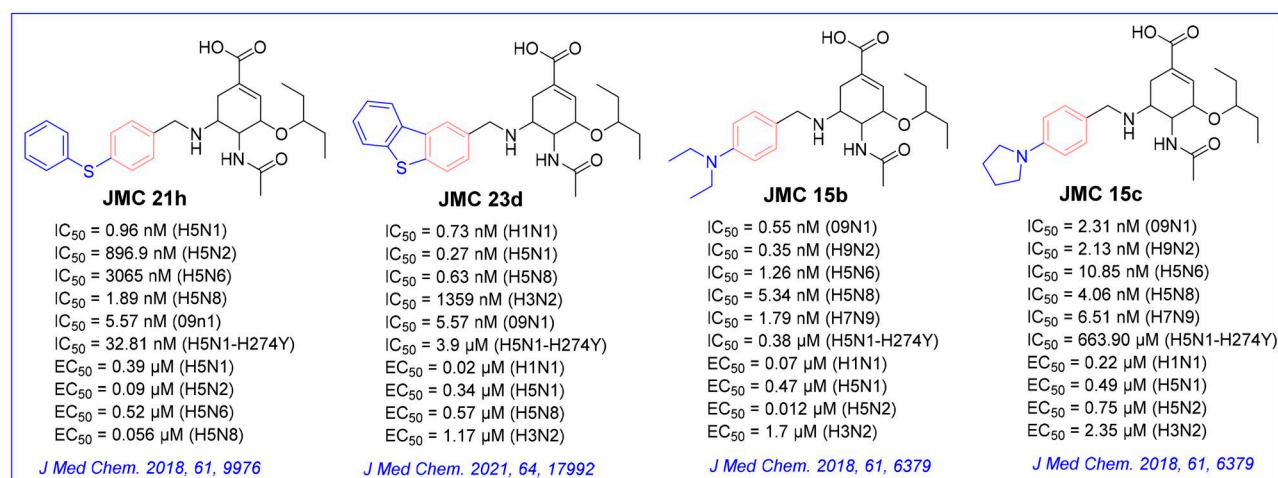
Figure 2. Comparison of the crystal structures of representative group-1 NAs (N1, PDB code: 2HU0, N8, PDB code 2HT7), group-2 NAs (N2, PDB code 4GZP), and 09N1 (PDB code 3TI6).

NA subtypes can be categorised into two groups: group-1 (N1, N4, N5 and N8), and group-2 (N2, N3, N6, N7 and N9) according to the phylogenetic tree<sup>14</sup>. To the best of current crystal structure knowledge, the 150-loop, containing residues 147–152, adopts an open conformation among group-1 NAs, forming the 150-cavity (Figure 2)<sup>15</sup>. In contrast, in group-2 NAs, this loop is always closed<sup>16</sup>. Further studies indicated that the conformation of group-2 NAs can be induced to form open 150-cavity by neuraminidase inhibitors<sup>17</sup>. Therefore, a deeper understanding of the relationship between the catalytic site and 150-loop can provide a new strategy for designing new influenza antiviral drugs that target both sites at the same time.

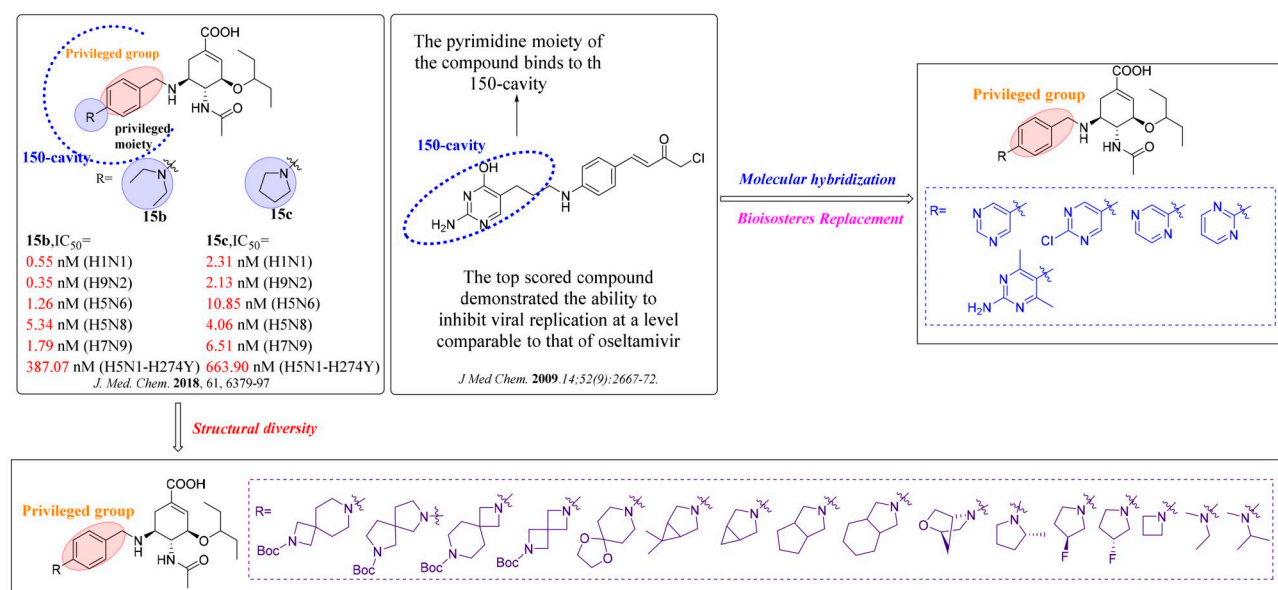
The crystal complex of NA-oseltamivir revealed that the C<sub>5</sub>-NH<sub>2</sub> group of oseltamivir is directed towards the 150-cavity, making such an amino group a potential modification site. Previous research efforts from our laboratory have identified several oseltamivir derivatives with more potent inhibitory activity than oseltamivir carboxylate (OSC, the active form of oseltamivir) against several subtypes of influenza virus (Figure 3)<sup>18–23</sup>. The discovery of these oseltamivir derivatives bearing different substituted benzyl groups indicated that it is reasonable to occupy 150-cavity with an appropriate substituent. Accordingly, a substituted benzyl group that mediates the hydrophobic force is a privileged moiety of the 150-cavity. Additional hydrophobic

interactions with the 150-cavity could improve the potency of these compounds against N1-H274Y mutants while retaining their outstanding potency against other group-1 NAs. In our recent screening, we identified compound **EJMC43b**<sup>20</sup> with the specific inhibition of group-1 NAs, which was a derivative of **JMC21h**. Although the inhibitory effect of these compounds was greatly improved, their inhibitory potency on group-2 NAs was robustly reduced. Unlike several compounds that were found to be selective group-1 NA inhibitors, compounds **JMC15b** and **JMC15c** showed potent inhibitory effects on both group-1 and group-2 NAs<sup>19</sup>. These results suggested that nitrogen-containing substituents such as polar groups or aromatic rings at the terminal end of benzene ring are capable to induce the open 150-cavity conformation and retain the potent inhibitory activity against group-2 NA.

Thus, to extend our previous work, we intended to introduce different *N*-substituted groups at the end of benzene ring to further explore the effects of substitutions on benzyl group. Herein, we designed and synthesised 21 novel oseltamivir analogues bearing enriched *N*-heterocycles substituents (Figure 4), anticipating that: (1) *N*-containing aryl groups, such as pyrimidine substituents at the para-position of the benzyl group, would bind effectively to the 150-cavity of group-1 NAs because of sufficiently large size, sufficient length, relative flexibility and hydrophobic force driving



**Figure 3.** Structures of our previously reported group-1-specific influenza NA inhibitors (JMC23d and JMC21h) and non-specific group-1 and group-2NA inhibitors (JMC15b and JMC15c).



**Figure 4.** The novel designed oseltamivir analogues *via* targeting the 150-cavity.

their binding; (2) the diverse *N*-heterocycles substitutions such as spiro substituents, bridge-ring substituents and cycloalkane substituents can induce the open 150-cavity conformation; (3) the introduction of different *N*-heterocycles substitutions could increase the Fsp<sup>3</sup> value to improve “drug-likeness” of the newly designed oseltamivir derivatives.

## Materials and methods

### Chemistry

The key chemical reactant oseltamivir phosphate was provided by Shandong Qidu Pharmaceutical Co., Ltd (Zibo, China). Other chemical materials were obtained from Bidepharmatech. Ltd (Shanghai, China) and were at least 97% pure. Solvents were obtained from Fuyuyq Co., Ltd (Tianjin, China). Thin-layer chromatography (TLC) was performed using plates coated with Silica Gel GF254 (SKU: 1077301000) for TLC (Merck, Shanghai, China), and the product spots were visualised under irradiation with UV light (l ¼ 254 nm). Flash column chromatography was conducted on columns packed

with Silica Gel (200e300 mesh, catalogue numbers: C0583530035), purchased from Qingdao Haiyang Chemical Company (Qingdao, China). Melting points (mp) of all compounds were measured with a micro melting point apparatus (RY-1G, Tianjin TianGuang Optical Instruments) without correction. <sup>1</sup>H NMR and <sup>13</sup>C NMR spectra were recorded on a Bruker AV-400 spectrometer with TMS as an internal standard and CD<sub>3</sub>OD or DMSO-*d*<sub>6</sub> as a solvent. Coupling constants (J) were expressed in hertz (Hz), and chemical shifts were reported in values (ppm) from TMS. Mass spectra (MS) were registered with API 4000 LC/MS spectrometer (Applied Biosystems, USA).

### General procedure for the preparation of compounds 1a~1e

Compounds **1a**~**1e** were obtained by Suzuki reaction of 4-formylphenylboronic acid with corresponding substituted aryl bromides. The reaction was monitored by TLC. To a solution of 4-formylphenylboronic acid (1.04 g, 6.93 mmol, 1.1 equiv), K<sub>3</sub>PO<sub>4</sub> (4.7 g, 22.05 mmol, 3.5 equiv), Pd(PPh<sub>3</sub>)<sub>4</sub> (0.7 g, 0.63 mmol, 0.1 equiv), N<sub>2</sub>,

in PhMe/H<sub>2</sub>O = 25/2 (30 ml) was added corresponding substituted aryl bromides (1 equiv). The reaction mixture was stirred under a nitrogen atmosphere at 100 °C for 12 h. Then, toluene was removed under reduced pressure, and brine (30 ml) was added. The mixture was extracted with ethyl acetate (3 × 30 ml), dried over anhydrous MgSO<sub>4</sub>, and concentrated *in vacuo* to give the crude product, which was purified by silica gel chromatography with ethyl acetate/petroleum ether (1:100) as the eluent to provide intermediates **1a~1e**.

#### General procedure for the preparation of compounds **2a~2e**

Via Borch reduction reaction, compounds **2a~2e** were synthesised from oseltamivir phosphate and an aldehyde (**1a~1e**). A mixture of oseltamivir phosphate (0.82 g, 2.0 mmol) and an aldehyde (**1a~1e**) (2.0 mmol, 1 eq) in 30 ml methanol was stirred at room temperature for 0.5 h, NaBH<sub>3</sub>CN (0.15 g, 2.5 mmol, 2.5 equiv) was added slowly. The reaction mixture was stirred at room temperature for 6–7 h. After the reaction completed (judged by TLC), methanol was evaporated in vacuum, and then, brine (30 ml) and saturated sodium carbonate solution (10 ml) were added. This mixture was extracted with ethyl acetate (3 × 30 ml), dried over anhydrous MgSO<sub>4</sub>, and concentrated under reduced pressure to give the crude product, which was purified by silica gel column chromatography with petroleum ether/ethyl acetate (1/1) and ethyl acetate to obtain the intermediates **2a~2e**.

#### General procedure for the preparation of compounds **3a~3e**

Compounds **3a~3e** were prepared by direct hydrolysis of the intermediates **2a~2e**. Each intermediate of **2a~2e** (1.0 mmol) was dissolved in 30 ml of methanol, and 1 M NaOH aqueous solution (5 ml) was added. The mixture was stirred at room temperature for 2 h. After that, most methanol was removed under reduced pressure and the residue was dissolved with 30 ml water. The aqueous phase was acidified (pH to 2–3) by 3 M HCl to precipitate the target compounds **3a~3e** which were collected by filtration and dried *in vacuo*.

#### (3R,4R,5S)-4-acetamido-3-(pentan-3-yloxy)-5-((4-(pyrimidin-5-yl)benzyl)amino)cyclohex-1-ene-1-carboxylic acid (**3a**)

White power, 83% yield, mp: 150–151 °C. <sup>1</sup>H NMR (600 MHz, CD<sub>3</sub>OD) δ: 9.16 (s, 1H, Pyrazine-H), 8.70 (d, *J* = 2.2 Hz, 1H, Pyrazine-H), 8.58 (s, 1H, Pyrazine-H), 8.20 (d, *J* = 8.0 Hz, 2H, 2Ph-H), 7.68 (d, *J* = 7.9 Hz, 2H, 2Ph-H), 6.89 (s, 1H, CH), 4.50 (d, *J* = 13.1 Hz, 1H, CH), 4.37 (d, *J* = 13.1 Hz, 1H, CH), 4.31–4.18 (*m*, 2H, 2CH), 3.74–3.64 (*m*, 1H, CH), 3.50–3.43 (*m*, 1H, CH), 3.08 (dd, *J* = 17.3, 5.3 Hz, 1H, CH), 2.75–2.66 (*m*, 1H, CH), 2.08 (s, 3H, CH<sub>3</sub>), 1.62–1.47 (*m*, 4H, 2CH<sub>2</sub>), 0.92 (dt, *J* = 12.4, 7.4 Hz, 6H, 2CH<sub>3</sub>). <sup>13</sup>C NMR (150 MHz, CD<sub>3</sub>OD) δ: 151.87, 144.46, 143.19, 141.83, 137.37, 132.61, 130.30, 127.44, 82.36, 74.55, 68.71, 55.15, 51.59, 25.86, 25.74, 25.26, 22.08, 21.70, 8.41, 8.17. ESI-MS: *m/z* 453.15 [M + H]<sup>+</sup>, C<sub>25</sub>H<sub>32</sub>N<sub>4</sub>O<sub>4</sub> (452.56).

#### (3R,4R,5S)-4-acetamido-3-(pentan-3-yloxy)-5-((4-(pyrimidin-5-yl)benzyl)amino)cyclohex-1-ene-1-carboxylic acid (**3b**)

White power, 81% yield, mp: 150–151 °C. <sup>1</sup>H NMR (400 MHz, Methanol-*d*<sub>4</sub>) δ: 8.87 (d, *J* = 4.8 Hz, 2H, 2 Pyrimidine-H), 8.50 (d, *J* = 7.7 Hz, 2H, 2Ph-H), 7.64 (d, *J* = 7.9 Hz, 2H, 2Ph-H), 7.40 (t, *J* = 4.8 Hz, 1H, Pyrimidine-H), 6.88 (s, 1H, CH), 4.49 (d, *J* = 12.7 Hz, 1H, CH), 4.41–4.19 (*m*, 3H, 3CH), 3.71 (*q*, *J* = 6.2, 5.8 Hz, 1H, CH),

3.47 (*p*, *J* = 5.5 Hz, 1H, CH), 3.08 (d, *J* = 18.3 Hz, 1H, CH), 2.77–2.63 (*m*, 1H, CH), 2.08 (s, 3H, CH<sub>3</sub>), 1.54 (dq, *J* = 13.5, 6.9 Hz, 4H, 2CH<sub>2</sub>), 0.91 (*q*, *J* = 7.6 Hz, 6H, 2CH<sub>3</sub>). <sup>13</sup>C NMR (150 MHz, CD<sub>3</sub>OD) δ: 163.47, 157.46, 138.66, 137.35, 133.37, 129.80, 128.55, 119.80, 82.36, 74.58, 55.16, 51.57, 25.90, 25.73, 25.25, 22.07, 8.41, 8.17. ESI-MS: *m/z* 453.15 [M + H]<sup>+</sup>, C<sub>25</sub>H<sub>32</sub>N<sub>4</sub>O<sub>4</sub> (452.56).

#### (3R,4R,5S)-4-acetamido-3-(pentan-3-yloxy)-5-((4-(pyrimidin-5-yl)benzyl)amino)cyclohex-1-ene-1-carboxylic acid (**3c**)

White power, 72% yield, mp: 132–133 °C. <sup>1</sup>H NMR (400 MHz, CD<sub>3</sub>OD) δ: 9.31–8.96 (*m*, *J* = 23.8, 9.8 Hz, 3H, 3Pyrimidine-H), 7.81 (d, *J* = 8.2 Hz, 2H, 2Ph-H), 7.64 (d, *J* = 8.2 Hz, 2H, 2Ph-H), 6.76 (s, 1H, CH), 4.30 (d, *J* = 13.3 Hz, 1H, CH), 4.23–4.00 (*m*, 3H, 3CH), 3.81–3.59 (*m*, 1H, CH), 3.45 (dt, *J* = 11.3, 5.5 Hz, 1H, CH), 2.97 (dd, *J* = 17.6, 5.2 Hz, 1H, CH), 2.59–2.45 (*m*, 1H, CH), 2.06 (s, 3H, CH<sub>3</sub>), 1.62–1.47 (*m*, 4H, 2CH<sub>2</sub>), 0.99–0.85 (*m*, 6H, 2CH<sub>3</sub>). <sup>13</sup>C NMR (100 MHz, CD<sub>3</sub>OD) δ: 173.09, 169.72, 156.75, 154.72, 135.36, 134.83, 134.19, 133.95, 130.44, 130.10, 127.28, 82.08, 75.12, 68.71, 54.83, 52.82, 27.81, 25.78, 25.24, 21.69, 8.46, 8.19. ESI-MS: *m/z* 453.39 [M + H]<sup>+</sup>, C<sub>25</sub>H<sub>32</sub>N<sub>4</sub>O<sub>4</sub> (452.56).

#### (3R,4R,5S)-4-acetamido-5-((4-(2-chloropyrimidin-5-yl)benzyl)amino)-3-(pentan-3-yloxy)cyclohex-1-ene-1-carboxylic acid (**3d**)

Yellow power, 78% yield, mp: 162–163 °C. <sup>1</sup>H NMR (400 MHz, CD<sub>3</sub>OD) δ: 8.83 (s, 2H, 2Pyrimidine-H), 7.67 (d, *J* = 8.0 Hz, 2H, 2Ph-H), 7.54 (d, *J* = 7.9 Hz, 2H, 2-Ph-H), 6.66 (s, 1H, CH), 4.18 (d, *J* = 13.2 Hz, 1H, CH), 4.11–4.06 (*m*, 2H, 2CH), 4.05–3.97 (*m*, 2H, 2CH), 3.41 (t, *J* = 5.6 Hz, 1H, CH), 2.92 (dd, *J* = 17.6, 5.3 Hz, 1H, CH), 2.44 (dd, *J* = 17.3, 9.3 Hz, 1H, CH), 2.02 (s, 3H, CH<sub>3</sub>), 1.57–1.47 (*m*, 4H, 2CH<sub>2</sub>), 0.90 (*q*, *J* = 7.5 Hz, 6H, 2CH<sub>3</sub>). <sup>13</sup>C NMR (100 MHz, DMSO-*d*<sub>6</sub>) δ: 172.69, 164.13, 156.47, 135.86, 134.43, 130.62, 129.81, 129.73, 129.67, 126.61, 126.11, 81.49, 73.86, 67.91, 53.54, 51.00, 25.43, 24.93, 24.42, 20.88, 7.62, 7.37. ESI-MS: *m/z* 487.53 [M + H]<sup>+</sup>, C<sub>25</sub>H<sub>31</sub>ClN<sub>4</sub>O<sub>4</sub> (487.00).

#### (3R,4R,5S)-4-acetamido-5-((4-(2-amino-4,6-dimethylpyrimidin-5-yl)benzyl)amino)-3-(pentan-3-yloxy)cyclohex-1-ene-1-carboxylic acid (**3e**)

White power, 71% yield, mp: 188–190 °C. <sup>1</sup>H NMR (400 MHz, CD<sub>3</sub>OD) δ: 7.46 (d, *J* = 7.9 Hz, 2H, 2Ph-H), 7.30 (d, *J* = 8.3 Hz, 2H, 2Ph-H), 6.47 (s, 1H, CH), 4.41–4.33 (*m*, 1H, CH), 3.90–3.80 (*m*, 3H, 3CH), 3.66 (*m*, 1H, CH), 3.43–3.32 (*m*, 1H), 2.92 (ddt, *J* = 12.3, 5.9, 0.9 Hz, 1H), 2.69 (s, 6H), 2.51 (ddt, *J* = 12.5, 3.1, 1.0 Hz, 1H), 1.95 (s, 3H), 1.61–1.48 (*m*, 4H, 2CH<sub>2</sub>), 0.93 (t, *J* = 7.2 Hz, 6H, 2CH<sub>3</sub>). <sup>13</sup>C NMR (100 MHz, DMSO-*d*<sub>6</sub>) δ: 173.50, 165.67, 139.89, 136.75, 135.03, 130.67, 130.15, 130.07, 129.56, 127.62, 127.55, 82.33, 74.69, 55.26, 51.67, 26.22, 25.75, 25.25, 22.08, 21.61, 21.32, 21.23, 8.44, 8.18. ESI-MS: *m/z* 496.22 [M + H]<sup>+</sup>, C<sub>27</sub>H<sub>37</sub>N<sub>5</sub>O<sub>4</sub> (495.62).

#### General procedure for the preparation of compounds **4a~4p**

Compounds **4a~4p** were prepared by electrophilic substitution reaction of corresponding amines with 4-fluorobenzaldehyde. Corresponding amines (10 mmol, 1.0 equiv) and K<sub>2</sub>CO<sub>3</sub> (2.76 g, 20 mmol, 2.0 equiv) were added to DMF (25 ml), and the mixture was heated at 100 °C for 0.5 h. Sequentially, 4-fluorobenzaldehyde (1.24 g, 10 mmol, 1.0 equiv) was added and the reaction was continued for 12 h at 100 °C. The mixture was poured into water and extracted with ethyl acetate (3 × 40 ml). The combined ethyl acetate solution was washed with brine (2 × 30 ml), dried over anhydrous MgSO<sub>4</sub> and concentrated to give the crude product.

Purification by column chromatography with a gradient of ethyl acetate/petroleum ether (1/50 to 1/10) as the eluent gave the corresponding compounds **4a~4p**.

#### General procedure for the preparation of compounds **5a~5p**

The synthetic procedures of **5a~5p** were similar to that of **2a~2e**, starting from intermediates **4a~4p**.

#### General procedure for the preparation of compounds **6a~6p**

The synthetic procedures of **6a~6p** were similar to that of **3a~3e**, starting from intermediates **5a~5p**.

#### (3*R*,4*R*,5*S*)-4-acetamido-5-((4-(2-(tert-butoxycarbonyl)-2,7-diazaspiro[3.5]nonan-7-yl)benzyl)amino)-3-(pentan-3-yloxy)cyclohex-1-ene-1-carboxylic acid (**6a**)

White power, 76% yield, mp: 156–158 °C. <sup>1</sup>H NMR (400 MHz, CD<sub>3</sub>OD) δ: 7.31 (d, *J* = 8.5 Hz, 2H, 2Ph-H), 7.01 (d, *J* = 8.5 Hz, 2H, 2Ph-H), 6.71 (s, 1H, CH), 4.23 (d, *J* = 13.0 Hz, 1H, CH), 4.19–4.03 (m, 3H, 3CH), 3.67 (s, 4H, 2CH<sub>2</sub>), 3.49–3.38 (m, *J* = 10.8, 5.3 Hz, 2H, 2CH), 3.26–3.11 (m, 4H, 2CH<sub>2</sub>), 2.96 (dd, *J* = 17.8, 4.8 Hz, 1H, CH), 2.58 (dd, *J* = 17.5, 9.3 Hz, 1H, CH), 2.03 (s, 3H, CH<sub>3</sub>), 1.92–1.81 (m, 4H, 2CH<sub>2</sub>), 1.57–1.48 (m, 4H, 2CH<sub>2</sub>), 1.44 (s, 9H, 3CH<sub>3</sub>), 0.89 (dd, *J* = 13.3, 7.3 Hz, 6H, 2CH<sub>3</sub>). <sup>13</sup>C NMR (100 MHz, CD<sub>3</sub>OD) δ: 173.29, 156.95, 152.11, 133.94, 130.53, 121.11, 116.22, 82.11, 79.61, 74.77, 54.48, 51.75, 47.90, 47.68, 45.83, 34.54, 33.15, 27.27, 25.76, 25.18, 21.91, 8.45, 8.16. ESI-MS: *m/z* 598.92 [M + H]<sup>+</sup>, C<sub>33</sub>H<sub>50</sub>N<sub>4</sub>O<sub>6</sub> (598.79).

#### (3*R*,4*R*,5*S*)-4-acetamido-5-((4-(7-(tert-butoxycarbonyl)-2,7-diazaspiro[4.4]nonan-2-yl)benzyl)amino)-3-(pentan-3-yloxy)cyclohex-1-ene-1-carboxylic acid (**6b**)

White power, 74% yield, mp: 160–161 °C. <sup>1</sup>H NMR (400 MHz, CD<sub>3</sub>OD) δ: 7.28 (d, *J* = 8.4 Hz, 2H, 2Ph-H), 6.80 (s, 1H, CH), 6.60 (d, *J* = 8.5 Hz, 2H, 2Ph-H), 4.25 (d, *J* = 13.0 Hz, 1H, CH), 4.21–4.07 (m, *J* = 19.0, 10.5 Hz, 3H, 3CH), 3.53–3.34 (m, 7H, 3CH<sub>2</sub>, CH), 3.27–3.20 (m, *J* = 6.6 Hz, 2H, CH<sub>2</sub>), 2.99 (dd, *J* = 17.4, 5.3 Hz, 1H, CH), 2.61 (dd, *J* = 17.1, 9.6 Hz, 1H, CH), 2.04 (s, 3H, CH<sub>3</sub>), 2.03–1.89 (m, 4H, 2CH<sub>2</sub>), 1.58–1.42 (m, 14H, 3CH<sub>3</sub>, 2CH<sub>2</sub>, CH), 0.90 (*q*, *J* = 7.3 Hz, 6H, 2CH<sub>3</sub>). <sup>13</sup>C NMR (100 MHz, CD<sub>3</sub>OD) δ: 173.40, 155.10, 148.68, 136.61, 130.73, 127.90, 111.63, 82.28, 79.60, 74.49, 66.74, 54.05, 51.48, 47.68, 46.56, 34.26, 27.36, 25.96, 25.72, 25.22, 21.97, 8.41, 8.14. ESI-MS: *m/z* 599.21 [M + H]<sup>+</sup>, C<sub>33</sub>H<sub>50</sub>N<sub>4</sub>O<sub>6</sub> (598.79).

#### (3*R*,4*R*,5*S*)-4-acetamido-5-((4-(7-(tert-butoxycarbonyl)-2,7-diazaspiro[3.5]nonan-2-yl)benzyl)amino)-3-(pentan-3-yloxy)cyclohex-1-ene-1-carboxylic acid (**6c**)

White power, 80% yield, mp: 157–158 °C. <sup>1</sup>H NMR (400 MHz, CD<sub>3</sub>OD) δ: 7.28 (d, *J* = 8.4 Hz, 2H, 2Ph-H), 6.78 (s, 1H, CH), 6.50 (d, *J* = 8.4 Hz, 2H, 2Ph-H), 4.25 (d, *J* = 13.0 Hz, 1H, CH), 4.14 (dd, *J* = 18.2, 10.5 Hz, 3H, 3CH), 3.64 (s, 4H, 2CH<sub>2</sub>), 3.52–3.38 (m, 6H, 3CH<sub>2</sub>), 2.98 (dd, *J* = 17.5, 5.3 Hz, 1H, CH), 2.60 (dd, *J* = 17.2, 9.5 Hz, 1H, CH), 2.04 (s, 3H, CH<sub>3</sub>), 1.77 (dd, *J* = 11.7, 6.3 Hz, 4H, 2CH<sub>2</sub>), 1.53 (dq, *J* = 14.0, 7.1 Hz, 4H, 2CH<sub>2</sub>), 1.46 (s, 9H, 3CH<sub>3</sub>), 0.90 (*q*, *J* = 7.2 Hz, 6H, 2CH<sub>3</sub>). <sup>13</sup>C NMR (100 MHz, CD<sub>3</sub>OD) δ: 173.39, 168.88, 155.16, 152.59, 135.40, 130.57, 129.22, 118.39, 111.27, 82.22, 79.74, 74.71, 61.03, 54.25, 51.58, 47.90, 35.20, 34.40, 27.29, 26.32, 25.73, 25.19, 22.00, 8.45, 8.17. ESI-MS: *m/z* 598.80 [M + H]<sup>+</sup>, C<sub>33</sub>H<sub>50</sub>N<sub>4</sub>O<sub>6</sub> (598.79).

#### (3*R*,4*R*,5*S*)-4-acetamido-5-((4-(6-(tert-butoxycarbonyl)-2,6-diazaspiro[3.3]heptan-2-yl)benzyl)amino)-3-(pentan-3-yloxy)cyclohex-1-ene-1-carboxylic acid (**6d**)

White power, 79% yield, mp: 155–156 °C. <sup>1</sup>H NMR (400 MHz, Methanol-*d*<sub>4</sub>) δ: 7.28 (d, *J* = 7.9 Hz, 2H, 2Ph-H), 6.75 (s, 1H, CH), 6.51 (d, *J* = 7.8 Hz, 2H, 2Ph-H), 4.23 (d, *J* = 12.9 Hz, 1H, CH), 4.19–4.13 (m, 2H, 2CH), 4.13–4.03 (m, 5H, CH, 2CH<sub>2</sub>), 3.97 (s, 4H, 2CH<sub>2</sub>), 3.51–3.39 (m, 2H, 2CH), 2.96 (dd, *J* = 17.4, 4.7 Hz, 1H, CH), 2.59 (dd, *J* = 17.4, 9.1 Hz, 1H, CH), 2.03 (s, 3H, CH<sub>3</sub>), 1.54 (dq, *J* = 13.2, 6.5 Hz, 4H, 2CH<sub>2</sub>), 1.44 (s, 9H, 3CH<sub>3</sub>), 0.90 (*q*, *J* = 6.7 Hz, 6H, 2CH<sub>3</sub>). <sup>13</sup>C NMR (100 MHz, Methanol-*d*<sub>4</sub>) δ: 173.28, 169.33, 156.54, 152.31, 134.58, 130.47, 129.85, 119.40, 111.81, 82.14, 79.76, 74.60, 61.56, 54.37, 51.62, 48.10, 47.73, 33.34, 27.23, 26.44, 25.75, 25.19, 21.90, 8.42, 8.14. ESI-MS: *m/z* 570.94 [M + H]<sup>+</sup>, C<sub>31</sub>H<sub>46</sub>N<sub>4</sub>O<sub>6</sub> (570.73).

#### (3*R*,4*R*,5*S*)-5-((4-(1,4-dioxo-8-azaspiro[4.5]decan-8-yl)benzyl)amino)-4-acetamido-3-(pentan-3-yloxy)cyclohex-1-ene-1-carboxylic acid (**6e**)

Brown power, 65% yield, mp: 131–133 °C. <sup>1</sup>H NMR (400 MHz, CD<sub>3</sub>OD) δ: 7.30 (d, *J* = 8.6 Hz, 2H, 2Ph-H), 7.00 (d, *J* = 8.6 Hz, 2H, 2Ph-H), 6.62 (s, 1H, CH), 4.21–4.03 (m, 4H, 4CH), 3.97 (s, 4H, 2CH<sub>2</sub>), 3.42 (t, *J* = 5.6 Hz, 1H, CH), 3.38–3.33 (m, 4H, 2CH<sub>2</sub>), 3.31 (s, 1H, CH), 2.99–2.90 (m, 1H, CH), 2.59–2.48 (m, 1H, CH), 2.02 (s, 3H, CH<sub>3</sub>), 1.80–1.74 (m, 4H, 2CH<sub>2</sub>), 1.57–1.47 (m, 4H, 2CH<sub>2</sub>), 0.89 (*q*, *J* = 7.3 Hz, 6H, 2CH<sub>3</sub>). <sup>13</sup>C NMR (100 MHz, DMSO-*d*<sub>6</sub>) δ: 173.44, 151.54, 136.43, 131.05–130.48 (m), 120.17, 115.91, 106.77, 82.28, 74.68, 63.97, 54.37, 51.52, 33.83, 26.11, 25.72, 25.21, 22.02, 8.45, 8.17. ESI-MS: *m/z* 516.6 [M + H]<sup>+</sup>, C<sub>28</sub>H<sub>41</sub>N<sub>3</sub>O<sub>6</sub> (515.65).

#### (3*R*,4*R*,5*S*)-4-acetamido-5-((4-(6,6-dimethyl-3-azabicyclo[3.1.0]hexan-3-yl)benzyl)amino)-3-(pentan-3-yloxy)cyclohex-1-ene-1-carboxylic acid (**6f**)

White power, 65% yield, mp: 143–145 °C. <sup>1</sup>H NMR (400 MHz, CD<sub>3</sub>OD) δ: 7.25 (d, *J* = 8.4 Hz, 2H, 2Ph-H), 6.62 (s, 1H, CH), 6.50 (d, *J* = 8.4 Hz, 2H, 2Ph-H), 4.26–3.98 (m, 4H, 4CH), 3.46–3.33 (m, 4H, 2CH<sub>2</sub>), 3.24 (d, *J* = 9.8 Hz, 2H, CH<sub>2</sub>), 2.96 (dd, *J* = 17.4, 5.0 Hz, 1H, CH), 2.57 (dd, *J* = 17.4, 9.4 Hz, 1H, CH), 2.02 (s, 3H, CH<sub>3</sub>), 1.59–1.44 (m, 6H, 2CH<sub>2</sub>, 2CH), 1.07 (s, 3H, CH<sub>3</sub>), 0.88 (dd, *J* = 13.5, 7.1 Hz, 6H, 2CH<sub>3</sub>), 0.84 (s, 3H, CH<sub>3</sub>). <sup>13</sup>C NMR (100 MHz, CD<sub>3</sub>OD) δ: 172.43, 171.00, 146.44, 131.75, 131.16, 129.81, 116.02, 110.52, 81.15, 74.14, 53.44, 50.94, 46.96, 26.755, 26.29, 24.95, 24.33, 21.06, 18.24, 10.27, 7.65, 7.35. ESI-MS: *m/z* 484.6 [M + H]<sup>+</sup>, C<sub>28</sub>H<sub>41</sub>N<sub>3</sub>O<sub>4</sub> (483.65).

#### (3*R*,4*R*,5*S*)-5-((4-(3-azabicyclo[3.1.0]hexan-3-yl)benzyl)amino)-4-acetamido-3-(pentan-3-yloxy)cyclohex-1-ene-1-carboxylic acid (**6g**)

White power, 72% yield, mp: 153–155 °C. <sup>1</sup>H NMR (400 MHz, CD<sub>3</sub>OD) δ: 7.25 (d, *J* = 8.2 Hz, 2H, 2Ph-H), 6.69 (s, 1H, CH), 6.58 (d, *J* = 8.2 Hz, 2H, 2Ph-H), 4.28–4.02 (m, 4H, 4CH), 3.55–3.36 (m, 4H, 4CH), 3.26–3.12 (m, 2H, CH<sub>2</sub>), 2.97–2.92 (m, 1H, CH), 2.65–2.52 (m, 1H, CH), 2.03 (s, 3H, CH<sub>3</sub>), 1.68 (dt, *J* = 7.4, 3.4 Hz, 2H, 2CH), 1.59–1.46 (m, 4H, 2CH<sub>2</sub>), 0.89 (dd, *J* = 7.1 Hz, 6H, 2CH<sub>3</sub>), 0.81–0.66 (m, 1H, CH), 0.30–0.19 (m, 1H, CH). <sup>13</sup>C NMR (100 MHz, CD<sub>3</sub>OD) δ: 173.32, 170.60, 149.39, 133.51, 131.16, 130.63, 117.26, 112.26, 112.16, 82.08, 74.92, 54.22, 51.71, 49.80, 39.13, 26.79, 25.76, 25.16, 21.97, 15.61, 9.70, 8.47, 8.18. ESI-MS: *m/z* 456.69 [M + H]<sup>+</sup>, C<sub>26</sub>H<sub>37</sub>N<sub>3</sub>O<sub>4</sub> (455.60).

**(3R,4R,5S)-4-acetamido-5-((4-(hexahydrocyclopenta[c]pyrrol-2(1H-yl)benzyl)amino)-3-(pentan-3-yloxy)cyclohex-1-ene-1-carboxylic acid (6h)**

White power, 63% yield, mp: 165–167 °C. <sup>1</sup>H NMR (400 MHz, CD<sub>3</sub>OD) δ: 7.27 (d, *J* = 8.2 Hz, 2H, 2Ph-H), 6.76 (s, 1H, CH), 6.64 (d, *J* = 8.3 Hz, 2H, 2Ph-H), 4.29–4.06 (m, 4H, 4CH), 3.52–3.44 (m, 1H, CH), 3.45–3.37 (m, 3H, 3CH), 3.05 (dd, *J* = 9.7, 3.3 Hz, 2H, CH<sub>2</sub>), 2.99 (dd, *J* = 17.3, 5.2 Hz, 1H, CH), 2.85–2.74 (m, 2H, 2CH), 2.66–2.55 (m, 1H, CH), 2.04 (s, 3H, CH<sub>3</sub>), 1.95–1.83 (m, 2H, 2CH), 1.80–1.67 (m, 1H, CH), 1.66–1.57 (m, 1H, CH), 1.57–1.46 (m, 6H, 6CH), 0.94–0.85 (m, 6H, 2CH<sub>3</sub>). <sup>13</sup>C NMR (100 MHz, CD<sub>3</sub>OD) δ: 173.37, 169.32, 149.54, 134.93, 130.60, 129.71, 117.19, 112.89, 82.17, 74.78, 54.69, 54.14, 51.61, 42.68, 32.61, 26.43, 25.74, 25.29, 25.18, 21.99, 8.46, 8.17. ESI-MS: *m/z* 482.29 [M - H]<sup>-</sup>, C<sub>28</sub>H<sub>41</sub>N<sub>3</sub>O<sub>4</sub> (483.65).

**(3R,4R,5S)-4-acetamido-5-((4-(octahydro-2H-isoindol-2-yl)benzyl)amino)-3-(pentan-3-yloxy)cyclohex-1-ene-1-carboxylic acid (6i)**

White power, 68% yield, mp: 147–148 °C. <sup>1</sup>H NMR (400 MHz, CD<sub>3</sub>OD) δ: 7.26 (d, *J* = 8.5 Hz, 2H, 2Ph-H), 6.63 (s, 1H, CH), 6.56 (d, *J* = 8.6 Hz, 2H, 2Ph-H), 4.22–4.07 (m, *J* = 15.4, 10.3 Hz, 3H, 3CH), 4.04 (d, *J* = 12.9 Hz, 1H, CH), 3.48–3.40 (m, 1H, CH), 3.31–3.28 (m, 1H, CH), 3.19 (dd, *J* = 9.1, 4.9 Hz, 2H, CH<sub>2</sub>), 2.97 (dd, *J* = 17.6, 5.3 Hz, 1H, CH), 2.63–2.51 (m, 1H, CH), 2.37 (dp, *J* = 11.7, 6.0 Hz, 2H, CH<sub>2</sub>), 2.04 (s, 3H, CH<sub>3</sub>), 1.83–1.13 (m, 14H, 6CH<sub>2</sub>, 2CH), 0.91 (dd, *J* = 13.2, 7.3 Hz, 6H, 2CH<sub>3</sub>). <sup>13</sup>C NMR (100 MHz, CD<sub>3</sub>OD) δ: 173.16, 172.29, 148.90, 133.10, 131.67, 130.47, 129.40, 117.04, 111.08, 110.54, 81.94, 75.17, 54.28, 52.08, 51.38, 37.26, 27.53, 25.99, 25.79, 25.15, 22.74, 21.90, 8.46, 8.17. ESI-MS: *m/z* 496.32 [M - H]<sup>-</sup>, C<sub>29</sub>H<sub>43</sub>N<sub>3</sub>O<sub>4</sub> (497.68).

**(3R,4R,5S)-4-acetamido-5-((4-(octahydro-2H-isoindol-2-yl)benzyl)amino)-3-(pentan-3-yloxy)cyclohex-1-ene-1-carboxylic acid (6j)**

Lavender power, 58% yield, mp: 147–148 °C. <sup>1</sup>H NMR (400 MHz, CD<sub>3</sub>OD) δ: 7.31 (d, *J* = 8.5 Hz, 2H, 2Ph-H), 6.86 (s, 1H, CH), 6.70 (d, *J* = 8.5 Hz, 2H, 2Ph-H), 4.68 (s, 1H, CH), 4.57 (s, 1H, CH), 4.37–4.07 (m, 4H, overlapped, 4CH), 3.83 (dd, *J* = 23.6, 7.2 Hz, 2H, CH<sub>2</sub>), 3.61–3.42 (m, 3H, overlapped, 3CH), 3.10 (d, *J* = 9.5 Hz, 1H, CH), 3.03 (dd, *J* = 17.5, 5.1 Hz, 1H, CH), 2.64 (dd, *J* = 17.3, 9.2 Hz, 1H, CH), 2.07 (s, 3H, CH<sub>3</sub>), 2.04–1.94 (m, *J* = 21.9, 5.4 Hz, 2H, CH<sub>2</sub>), 1.62–1.48 (m, 4H, 2CH<sub>2</sub>), 0.98–0.86 (m, 6H, 2CH<sub>3</sub>). <sup>13</sup>C NMR (100 MHz, CD<sub>3</sub>OD) δ: 172.60, 167.08, 147.48, 135.64, 130.04, 127.31, 116.84, 112.17, 81.48, 75.62, 73.79, 70.86, 56.97, 56.24, 53.44, 50.69, 47.08, 46.88, 35.42, 25.25, 24.91, 24.41, 21.18, 7.60, 7.34. ESI-MS: *m/z* 472.39 [M + H]<sup>+</sup>, C<sub>26</sub>H<sub>39</sub>N<sub>3</sub>O<sub>4</sub> (471.60).

**(3R,4R,5S)-4-acetamido-5-((4-((R)-2-methylpyrrolidin-1-yl)benzyl)amino)-3-(pentan-3-yloxy)cyclohex-1-ene-1-carboxylic acid (6k)**

White power, 79% yield, mp: 160–161 °C. <sup>1</sup>H NMR (400 MHz, CD<sub>3</sub>OD) δ: 7.27 (d, *J* = 7.9 Hz, 2H, 2Ph-H), 6.85–6.45 (m, *J* = 12.6 Hz, 3H, CH, 2Ph-H), 4.34–4.10 (m, 3H, 3CH), 4.07 (d, *J* = 12.8 Hz, 1H, CH), 3.95–3.86 (m, 1H, CH), 3.64–3.36 (m, 3H, CH, CH<sub>2</sub>), 3.17 (dd, *J* = 16.2, 8.0 Hz, 1H, CH), 3.08–2.87 (m, 1H, CH), 2.70–2.47 (m, 1H, CH), 2.24–1.88 (m, 6H, CH<sub>2</sub>, CH, CH<sub>3</sub>), 1.80–1.69 (m, 1H, CH), 1.64–1.44 (m, 4H, 2CH<sub>2</sub>), 1.16 (d, *J* = 6.1 Hz, 3H, CH<sub>3</sub>), 0.91 (dd, *J* = 12.0, 7.1 Hz, 6H, 2CH<sub>3</sub>). <sup>13</sup>C NMR (100 MHz, CD<sub>3</sub>OD) δ: 147.92, 130.62, 129.41, 127.95, 116.58, 111.82, 111.39, 81.99, 74.96, 54.30, 53.47, 51.83, 32.56, 25.77, 25.16, 22.71, 21.89, 17.86, 8.45, 8.16. ESI-MS: *m/z* 456.6 [M - H]<sup>-</sup>, C<sub>26</sub>H<sub>39</sub>N<sub>3</sub>O<sub>4</sub> (457.62).

**(3R,4R,5S)-4-acetamido-5-((4-((R)-2-methylpyrrolidin-1-yl)benzyl)amino)-3-(pentan-3-yloxy)cyclohex-1-ene-1-carboxylic acid (6l)**

White power, 58% yield, mp: 150–151 °C. <sup>1</sup>H NMR (400 MHz, CD<sub>3</sub>OD) δ: 7.27 (d, *J* = 7.9 Hz, 2H, 2Ph-H), 6.85–6.45 (m, *J* = 12.6 Hz, 3H, CH, 2Ph-H), 4.34–4.10 (m, 3H, 3CH), 4.07 (d, *J* = 12.8 Hz, 1H, CH), 3.95–3.86 (m, 1H, CH), 3.64–3.36 (m, 3H, CH, CH<sub>2</sub>), 3.17 (dd, *J* = 16.2, 8.0 Hz, 1H, CH), 3.08–2.87 (m, 1H, CH), 2.70–2.47 (m, 1H, CH), 2.24–1.88 (m, 6H, CH<sub>2</sub>, CH, CH<sub>3</sub>), 1.80–1.69 (m, 1H, CH), 1.64–1.44 (m, 4H, 2CH<sub>2</sub>), 1.16 (d, *J* = 6.1 Hz, 3H, CH<sub>3</sub>), 0.91 (dd, *J* = 12.0, 7.1 Hz, 6H, 2CH<sub>3</sub>). <sup>13</sup>C NMR (100 MHz, CD<sub>3</sub>OD) δ: 170.68, 148.36, 133.11, 130.73, 111.80, 82.04, 74.78, 54.27, 51.65, 47.82, 45.00, 31.92, 26.77, 25.76, 25.15, 21.88, 8.43, 8.14. ESI-MS: *m/z* 460.7 [M - H]<sup>-</sup>, C<sub>25</sub>H<sub>36</sub>FN<sub>3</sub>O<sub>4</sub> (461.59).

**(3R,4R,5S)-4-acetamido-5-((4-((R)-2-fluoropyrrolidin-1-yl)benzyl)amino)-3-(pentan-3-yloxy)cyclohex-1-ene-1-carboxylic acid (6m)**

White power, 63% yield, mp: 145–147 °C. <sup>1</sup>H NMR (400 MHz, CD<sub>3</sub>OD) δ: 7.30 (d, *J* = 8.6 Hz, 2H), 6.75 (s, 1H), 6.63 (d, *J* = 8.6 Hz, 2H), 5.38 (dt, *J* = 53.5, 3.8 Hz, 1H), 4.25 (d, *J* = 13.0 Hz, 1H), 4.20–4.07 (m, 3H), 3.65–3.53 (m, 1H), 3.51 (dd, *J* = 7.2, 3.5 Hz, 1H), 3.47–3.38 (m, 4H), 3.00 (dd, *J* = 17.5, 5.5 Hz, 1H), 2.65–2.55 (m, 1H), 2.33 (ddd, *J* = 18.6, 13.3, 5.4 Hz, 1H), 2.24–2.09 (m, 1H), 2.04 (s, 3H), 1.59–1.46 (m, 4H), 0.90 (q, *J* = 7.4 Hz, 6H). <sup>13</sup>C NMR (100 MHz, DMSO-*d*<sub>6</sub>) δ: 170.82, 167.73, 147.59, 137.65, 130.86, 128.96, 112.13, 81.48, 75.33, 54.09, 52.42, 45.67, 32.07, 26.04, 25.51, 23.76, 9.87, 9.35. ESI-MS: *m/z* 462.5 [M + H]<sup>+</sup>, C<sub>25</sub>H<sub>36</sub>FN<sub>3</sub>O<sub>4</sub> (461.58).

**(3R,4R,5S)-4-acetamido-5-((4-(azetidin-1-yl)benzyl)amino)-3-(pentan-3-yloxy)cyclohex-1-ene-1-carboxylic acid (6n)**

White power, 69% yield, mp: 156–158 °C. <sup>1</sup>H NMR (400 MHz, CD<sub>3</sub>OD) δ: 7.49–7.26 (m, 2H, 2Ph-H), 6.73 (s, 1H, CH), 6.61–6.38 (m, *J* = 8.4 Hz, 2H, 2Ph-H), 4.41–3.96 (m, *J* = 32.0, 29.2, 21.9 Hz, 4H, overlapped, 4CH), 3.92–3.83 (m, *J* = 11.5, 7.2 Hz, 3H, overlapped, 3CH), 3.82–3.64 (m, 1H, CH), 3.57–3.37 (m, 2H, CH<sub>2</sub>), 3.08–2.89 (m, 1H, CH), 2.57 (dd, *J* = 52.4, 21.8 Hz, 1H, CH), 2.47–2.24 (m, *J* = 14.9, 7.4 Hz, 2H, CH<sub>2</sub>), 2.05 (s, 3H, CH<sub>3</sub>), 1.62–1.45 (m, *J* = 15.4 Hz, 4H, 2CH<sub>2</sub>), 1.01–0.79 (m, *J* = 13.3, 7.3 Hz, 6H, 2CH<sub>3</sub>). <sup>13</sup>C NMR (100 MHz, CD<sub>3</sub>OD) δ: 153.05, 130.40, 127.94, 111.34, 82.06, 74.83, 68.71, 54.47, 52.45, 51.9, 51.75, 25.76, 25.17, 21.88, 21.68, 16.31, 8.43, 8.14. ESI-MS: *m/z* 429.91 [M + H]<sup>+</sup>, C<sub>24</sub>H<sub>35</sub>N<sub>3</sub>O<sub>4</sub> (429.56).

**(3R,4R,5S)-4-acetamido-5-((4-(ethyl(methyl)amino)benzyl)amino)-3-(pentan-3-yloxy)cyclohex-1-ene-1-carboxylic acid (6o)**

Yellow power, 66% yield, mp: 153–155 °C. <sup>1</sup>H NMR (400 MHz, DMSO-*d*<sub>6</sub>) δ: 7.26 (d, *J* = 8.5 Hz, 2H, 2Ph-H), 6.74 (d, *J* = 8.5 Hz, 2H, 2-Ph-H), 6.60 (s, 1H, CH), 4.21–3.98 (m, 4H, 4CH), 3.47–3.38 (m, 3H, 3CH), 3.36–3.32 (m, 1H, CH), 2.99–2.93 (m, 1H, CH), 2.91 (s, 3H, CH<sub>3</sub>), 2.54 (dd, *J* = 17.7, 9.2 Hz, 1H, CH), 2.02 (s, 3H, CH<sub>3</sub>), 1.58–1.44 (m, 4H, 2CH<sub>2</sub>), 1.09 (t, *J* = 7.0 Hz, 3H, CH<sub>3</sub>), 0.89 (q, *J* = 7.1 Hz, 6H, 2CH<sub>3</sub>). <sup>13</sup>C NMR (100 MHz, CD<sub>3</sub>OD) δ: 172.62, 149.09, 135.26, 129.95, 128.53, 115.86, 111.25, 81.44, 73.88, 53.32, 50.70, 35.82, 35.49, 25.38, 25.00, 24.91, 24.46, 24.38, 21.18, 9.10, 7.62, 7.35. ESI-MS: *m/z* 430.61 [M - H]<sup>-</sup>, C<sub>24</sub>H<sub>37</sub>N<sub>3</sub>O<sub>4</sub> (431.58).

**(3R,4R,5S)-4-acetamido-5-((4-((R)-2-fluoropyrrolidin-1-yl)benzyl)amino)-3-(pentan-3-yloxy)cyclohex-1-ene-1-carboxylic acid (6p)**

Yellow powder, 65% yield, mp: 141–143 °C. <sup>1</sup>H NMR (400 MHz, DMSO-*d*<sub>6</sub>) δ: 7.27 (d, *J* = 8.5 Hz, 2H, 2Ph-H), 6.82 (d, *J* = 8.4 Hz, 2H, 2Ph-H), 6.62 (s, 1H, CH), 4.25–3.98 (m, 5H, 5CH), 3.41 (p, *J* = 5.6 Hz, 1H, CH), 3.38–3.32 (m, 1H, CH), 2.96 (dd, *J* = 17.5, 5.4 Hz, 1H, CH), 2.73 (s, 3H, CH<sub>3</sub>), 2.63–2.51 (m, 1H, CH), 2.02 (s, 3H, CH<sub>3</sub>), 1.52 (td, *J* = 9.6, 8.9, 6.6 Hz, 4H, 2CH<sub>2</sub>), 1.15 (d, *J* = 6.6 Hz, 6H, 2CH<sub>3</sub>), 0.89 (q, *J* = 7.1 Hz, 6H, 2CH<sub>3</sub>). <sup>13</sup>C NMR (100 MHz, CD<sub>3</sub>OD) δ: 171.34, 169.13, 167.25, 132.03, 131.25, 128.02, 125.38, 81.57, 74.87, 54.41, 51.04, 45.31, 30.89, 26.04, 25.93, 25.47, 23.99, 9.86, 9.31. ESI-MS: *m/z* 446.11 [M + H]<sup>+</sup>, C<sub>25</sub>H<sub>39</sub>N<sub>3</sub>O<sub>4</sub> (445.60).

### Biological evaluation

#### Neuraminidase enzyme inhibitory assay *in vitro*

The influenza NA inhibition assay was performed as previously described<sup>21,24,26</sup>. Influenza viral suspensions of A/Goose/Guangdong/SH7/2013 (H5N1) and A/Duck/Guangdong/674/2014 (H5N6) were harvested from the allantoic fluid of influenza virus-infected chicken embryo layer, and A/PuertoRico/8/1934 (H1N1), A/Babol/36/2005 (H3N2) and A/Anhui/1/2005 (H5N1-H274Y) were obtained from Sino Biological Inc (Catalogue numbers: 40909-V08B, 40017-VNAHC and 11676-VNAHC1, respectively). NA inhibitory activities were examined by using a chemiluminescence-based assay with 2'-(4-methylumbelliferyl)- $\alpha$ -D-N-acetylneuraminic acid (MUNANA) as the substrate, which was cleaved by NA to provide a quantifiable fluorescent product. The tested compounds were dissolved in DMSO and diluted to the corresponding concentrations in MES buffer (1.27 g 2-(N-morpholino)ethanesulphonic acid and 0.09 g CaCl<sub>2</sub> in 200 ml Milli-Q water). Subsequently, 10  $\mu$ L of diluted virus supernatant or NA assay diluent, along with 70  $\mu$ L of MES buffer and 10  $\mu$ L of test compounds at varying concentrations, were sequentially added to a 96-well plate and incubated for 10 min at 37 °C. To start the reaction, 10  $\mu$ L of substrate was added to each well. Following a subsequent incubation period of 40 min, the reaction was stopped by adding 150  $\mu$ L of stopping solution (3 g glycine and 1.6 g NaOH in 200 ml Milli-Q water). At Ex = 365 nm and Em = 460 nm, fluorescence was measured with a microplate reader (Molecular Devices, SpectraMax iD5). The values of IC<sub>50</sub> (50%-inhibitory concentration) were obtained from the dose-response curves by plotting the percent inhibition of NA activity versus the concentration of the compounds.

#### *In vitro* anti-influenza virus assay and cytotoxicity assay in chicken embryo fibroblast (CEF)

The anti-influenza activity (EC<sub>50</sub>) and cytotoxicity (CC<sub>50</sub>) of the novel synthesised oseltamivir derivatives were determined with H5N1 and H5N6 strains in Chicken Embryo Fibroblasts (CEFs) (Extracted from 9-day-old chicken embryo eggs, provided by Institute of Poultry Science, Shandong Academy of Agricultural Sciences) utilising Cell Counting Kit-8 (CCK-8, Dojindo Laboratories) method as our previously described<sup>19,20,22,26</sup>. Chicken embryo fibroblasts (CEFs) were infected with H5N1 and H5N6 as an antiviral detection model to determine the inhibitory effect of these compounds on the cytopathic effect (CPE) induced by IFV. The tested compounds and positive control were dissolved in DMSO and diluted to the corresponding concentrations by 3-fold dilution in medium (1% FBS in DMEM). Aliquots of 50  $\mu$ L of diluted influenza viral suspension (H5N1, H5N6) were mixed with equal volumes of solutions of the novel synthesised compounds.

In 96-well plates, the mixtures were added to CEFs and then incubated at 37 °C under 5% CO<sub>2</sub> for 48 h. Then, 100  $\mu$ L per well of CCK-8 reagent solution (10  $\mu$ L of CCK-8 in 90  $\mu$ L of media) was added. After incubating at 37 °C for 90 min, the absorbance at 450 nm was read on a microplate reader. The EC<sub>50</sub> values were obtained by fitting the curve of percent CPE (cytopathic effect) versus inhibitor concentration. The values of CC<sub>50</sub> (50% cytotoxic concentration) of NA inhibitors to CEFs were determined similarly to the EC<sub>50</sub> but without virus infection.

#### Plaque reduction assay (PRA) in MDCK cells

The antiviral activity of selected compounds towards the H1N1 and H3N2 viruses was determined by PRA (plaque reduction assay). The procedure of this assay adhered to our recently published research and was conducted at the Department of Molecular Medicine, University of Padova<sup>20,27,28</sup>. Briefly, a confluent monolayer of MDCK cells (Madin-Darby Canine Kidney cells, from Department of Molecular Medicine, University of Padova) was seeded in 12-well plates. After incubating for 24 h at 37 °C, cells were infected with FluA virus (PR8 or WSN strain) at approximately 40 PFU/well in DMEM supplemented with 1  $\mu$ g/mL of TPCK-treated trypsin (Worthington Biochemical Corporation, catalogue numbers: LS02120) and 0.14% BSA (Sigma, catalogue numbers: A7906) for 1 h at 37 °C. After virus adsorption, the cells were overlaid with medium containing 1  $\mu$ g/mL TPCK-treated trypsin, 0.14% BSA, 1.2% Avicel cellulose and different concentrations of test compounds. Oseltamivir carboxylic acid (OSC) and zanamivir (ZAN) were included as reference compounds in each experiment. At 2 days post-infection, cells monolayers were fixed with 4% (v/v) formaldehyde and stained with 0.1% toluidine blue. Viral plaques were counted and the mean plaque number of DMSO-treated control group was set at 100% of plaque formation.

#### Cytotoxicity assay in MDCK cells

Cytotoxicity of representative compounds against MDCK cells was assessed by the 3-(4,5-dimethylthiazol-2-yl)-2,5-diphenyltetrazolium bromide (MTT) method as our previously reported<sup>29,30</sup>. MDCK cells (seeded at density of  $2 \times 10^4$  cells per well) were grown in 96-well plates for 24 h and then treated with serial dilutions of test compounds, or DMSO as a control, in DMEM supplemented with 10% FBS and 1% P/S. After incubation for 48 h at 37 °C, MTT solution (5 mg/ml in PBS) was added to each well, and plates were incubated at 37 °C for 4 h in a CO<sub>2</sub> incubator. Successively, a solubilisation solution (10% SDS, 0.01 N HCl) was added to lyse cells and incubated overnight at 37 °C. Finally, absorbance was read at the wavelength of 570 nm on a microtiter plate reader (MultiSkan FC, Thermo Scientific).

### *In silico* studies

#### Computational methods

The molecular docking was performed utilising Schrödinger Maestro 11.8 software. The molecular structures of compounds **6k** was optimised using LigPrep module. The stable conformer with minimum potential energy was generated via OPLS force field<sup>31</sup>.

The crystal structures of N1 (H1N1, PDB code: 3BEQ), N1 (2HU0), and N2 (H2N2, PDB code: 4K1K) were performed from the Protein Data Bank. The addition of hydrogen atoms and removal of unwanted water molecules were implemented using the "Protein Preparation Wizard" tool of Maestro 11.8<sup>32</sup>. Molecular docking of **6k** was carried out with standard Glide protocol



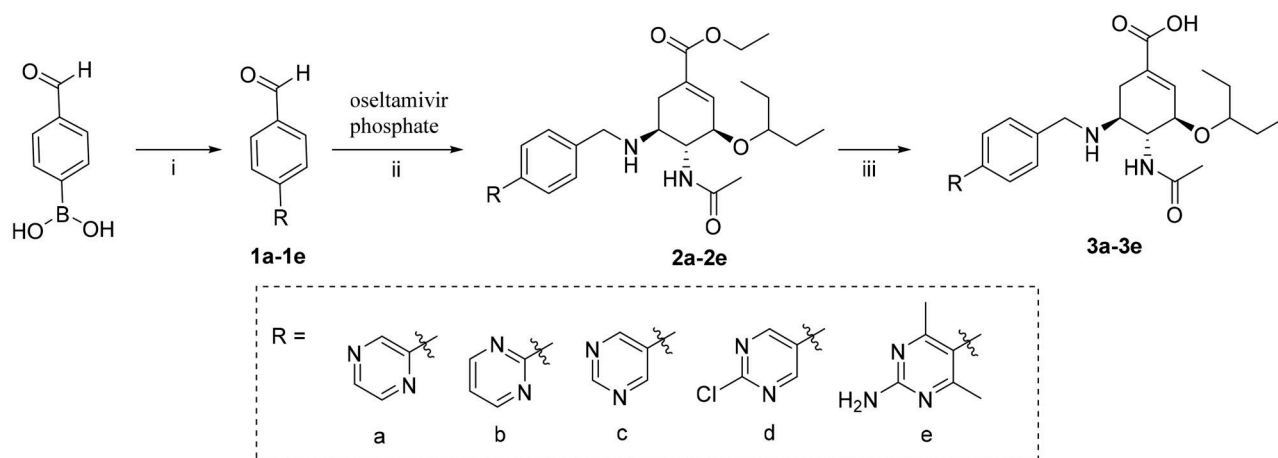
(Schrödinger Maestro 11.8)<sup>33</sup>. Docking results were visualised using the software of PyMOL version 1.5.

The system builder module was used to build the molecular dynamic simulation structure. The atomic framework had been solvated with Transferable Interatomic Potential with Three Points (TIP<sub>3</sub>P) crystallographic water particles with orthorhombic intermittent limit conditions. The minimum distance was set as 10 Å. After eliminating the overlapping water molecules, Na<sup>+</sup> or Cl<sup>-</sup> were added to neutralise the entire framework of atoms, and an extra 0.15 M NaCl was added into the system. With the NPT ensemble class of Nose-Hoover thermostat and barostat to maintain the constant temperature of 300 K and pressure of 1.013 bar in the system, the 200 ns productive simulation was performed. The protein backbone RMSD, ligand heavy atom RMSD, and RMSF plots were generated by analysing the resultant trajectory with Maestro.

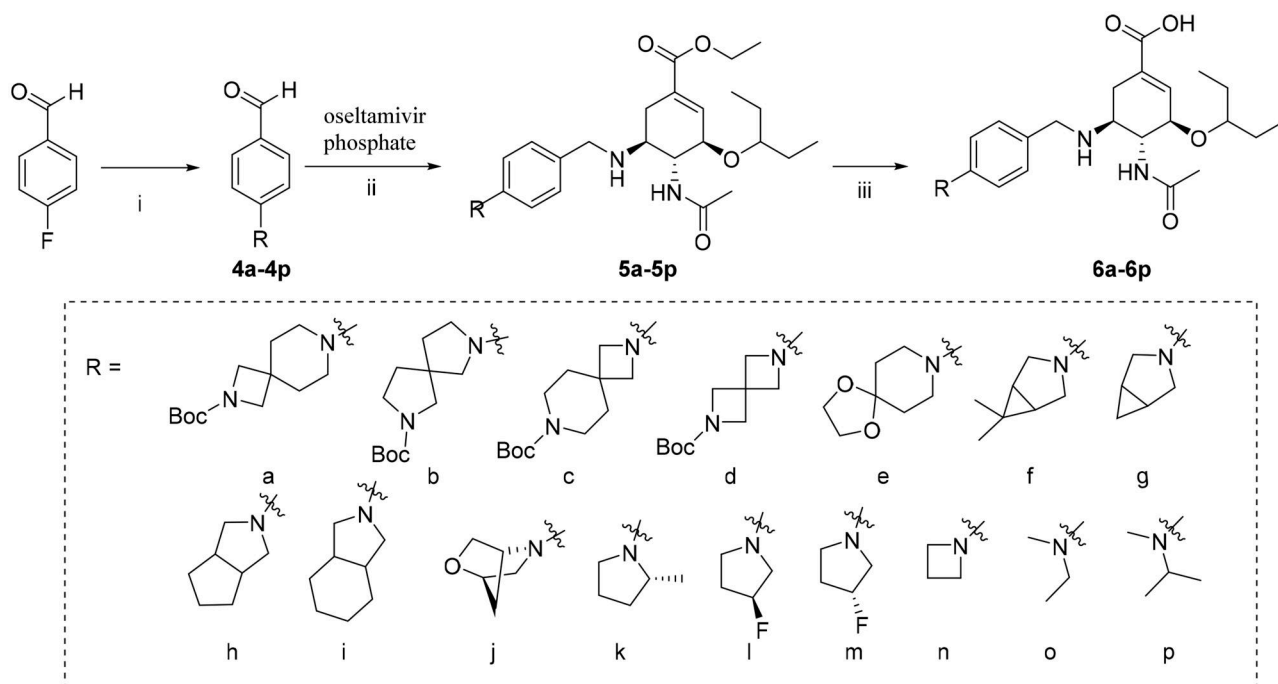
## Results and discussion

### Chemistry

The C-5 modified oseltamivir derivatives (**3a-3e**, **6a-6p**) were prepared via a concise and well-established synthetic route as outlined in **Scheme 1** and **Scheme 2**. As shown in **Scheme 1**, a Suzuki reaction of the (4-formylphenyl) boronic acid with the corresponding bromo-substituted aromatic heterocycle gave five substituted biphenyl benzaldehydes (**1a-1e**), which were used in synthesising intermediates **2a-2e**. Finally, the target compounds (**3a-3e**) were prepared by direct hydrolysis of the intermediates **2a-2e**. Compounds **6a-6p** were synthesised according to the synthetic protocols represented in **Scheme 2**. Compounds **4a-4p** were prepared by the reaction of corresponding amines with 4-fluorobenzaldehyde in the presence of potassium carbonate. Then,



**Scheme 1.** Reagents and conditions: (i) Corresponding bromo-substituted aromatic heterocycle, K<sub>3</sub>PO<sub>4</sub>, Pd(PPh<sub>3</sub>)<sub>4</sub>, N<sub>2</sub>, toluene/H<sub>2</sub>O = 25/2, 100 °C, 12 h; (ii) NaBH<sub>3</sub>CN, CH<sub>3</sub>OH, r.t., 6–7 h; (iii) 1 M NaOH, CH<sub>3</sub>OH, r.t., then 3 M HCl.



**Scheme 2.** Reagents and conditions: (i) Corresponding amine, K<sub>2</sub>CO<sub>3</sub>, DMF, 100 °C, 12 h; (ii) NaBH<sub>3</sub>CN, CH<sub>3</sub>OH, r.t., 6–7 h; (iii) 1 M NaOH, CH<sub>3</sub>OH, r.t., then 3 M HCl.

following a previously reported procedure, **4a-4p** were reacted with commercial oseltamivir phosphate in the presence of NaBH<sub>3</sub>CN to obtain the key intermediates **5a-5p**, which was followed by direct hydrolysis to afford the target compounds **6a-6p**.

### Biological evaluation

#### *In vitro* activities of influenza neuraminidase inhibitors

All the synthesised compounds were screened for their NA inhibitory activities using a chemiluminescence-based assay with 2'-(4-methylumbelliferyl)- $\alpha$ -D-N-acetylneuraminic acid (MUNANA) as the substrate<sup>19-23,25,34</sup>. We chose wild-type N1 (H1N1, H5N1) or mutated N1 (H5N1-H274Y) from group-1, N2 (H5N2) and N6 (H5N6) from group-2 as representatives for testing. OSC (Oseltamivir acid) and ZNA (Zanamivir) was selected as positive control drug. The inhibitory activities of the synthesised compounds and OSC are reported in Table 1. As a broad-spectrum neuraminidase inhibitor, OSC showed high inhibitory potency against all selected wild-type NAs with IC<sub>50</sub> values of 15 nM, 28 nM, 50 nM, and 16 nM against H1N1, H3N2, H5N1, and H5N6, respectively.

In the tested series, all oseltamivir derivatives showed decreased inhibitory activities against selected wild-type NAs. Among them, **3a-3e** with R group of pyrazinyl and pyrimidinyl exhibited a great decrease in inhibitory activity against H1N1 and H3N2 (IC<sub>50</sub> = 4.74–12.14  $\mu$ M). This confirmed our previous hypothesis that when electron-withdrawing substituents with higher electron cloud density were introduced into the dominant benzyl group targeting the 150-cavity hydrogen bond region, the activity of the compound decreased. In particular, when the nitrogen atom of the pyrimidine ring was at 3-position and 5-position (**3c-3e**), the absence of electron-donating conjugated effect of nitrogen atom on benzyl results in a more significant decrease in the electron cloud density of the benzyl group, which further reduced the inhibitory activity of compounds compared to **3a** and **3b**. Although the activity of **3a-3e** decreased, they displayed similar inhibitory activity against group-1 NAs and group-2 NAs, without selectivity.

Replacing terminal aromatic nitrogen-containing heterocycles with nitrogen-containing aliphatic heterocycles greatly improved the inhibitory activity of compounds **6a-6p** against NAs. Among them, **6k** with R group of (*r*)-2-methylpyrrole (IC<sub>50</sub> = 0.084  $\mu$ M) exhibited similar activities towards H1N1 compared to OSC (IC<sub>50</sub> = 0.015  $\mu$ M). As for the other wild-type NAs, **6k** was proved to have a strong inhibitory effect on both group-1 (H5N1, IC<sub>50</sub> = 0.23  $\mu$ M) and group-2 NAs (H3N2, IC<sub>50</sub> = 0.12  $\mu$ M; H5N6, IC<sub>50</sub> = 0.15  $\mu$ M) with similar activity or slightly weaker than that of OSC. The introduction of electron-withdrawing substituents on pyrrolidine groups was not conducive to an enhancement of activity, as seen with compounds **6l** and **6m** bearing 3-fluoropyrrole (H1N1, IC<sub>50</sub> = 0.23  $\mu$ M and 0.37  $\mu$ M, respectively; H3N2, IC<sub>50</sub> = 0.40  $\mu$ M and 0.43  $\mu$ M, respectively; H5N1, IC<sub>50</sub> = 0.69  $\mu$ M and 0.84  $\mu$ M, respectively; H5N6, IC<sub>50</sub> = 0.24  $\mu$ M and 0.18  $\mu$ M, respectively) and showing lower potency than **6k**.

Further strengthening the flexibility and size of R group is detrimental to the improvement of the inhibitory activity of compounds, such as **6a-6e** with R group of nitrogen-containing spiroheterocycles. More extensive hydrophobic interactions brought by relatively large size did not contribute to the activity, probably because the large size of R group may make the OSC nucleus deflect to a certain extent. In addition, by replacing spiro substituents with bicyclic or bridge-ring substituents, we obtained compounds **6f-6j** with more potent inhibitory activity than **6a-6e**. This

result demonstrated that conformational restriction by increasing the rigidity of substituents is beneficial to reinforce the compatibility of substituents with 150-cavity. Compounds **6f-6j** exhibited similar potency towards group-1 and group-2 NAs with IC<sub>50</sub> values of 0.14–0.59  $\mu$ M. In nitrogen-containing bicyclic derivatives (**6f-6i**), the size of the terminal cycloalkane substituent has little effect on the inhibitory activity.

Inspired by the result of **6k** and to further examine the size effects of *N*-substituted fragments, we performed ring contraction and ring opening for the pyrrole ring contained in **6k** to obtain compounds **6n-6p**. The activity results indicated that the more flexible conformation caused by the size reduction of substituents did not improve the inhibitory potency of compounds, which may be due to the fact that too small substituents cannot establish suitable hydrophobic interactions with surrounding amino acids to fully occupy 150-cavity. Among them, **6o** bearing *N,N*-dimethyl-ethylamine substituent displayed the lowest inhibitory activity (IC<sub>50</sub> = 0.36–0.89  $\mu$ M) against wild-type NAs compared with **6n** (IC<sub>50</sub> = 0.14–0.42  $\mu$ M) and **6p** (IC<sub>50</sub> = 0.17–0.52  $\mu$ M). Compound **6p** showed improved activities by introducing methyl on *N,N*-dimethyl-ethylamine substituent.

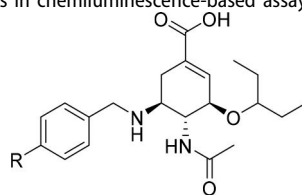
Overall, *N*-heterocycles substituted oseltamivir derivatives have been shown to have broad-spectrum inhibitory activity on group-1 and group-2 NAs. Consistently with our previous results, the NA inhibitory activity of novel *N*-heterocycles substituted oseltamivir derivatives is very sensitive to the flexibility, size and hydrophobicity of R group<sup>19</sup>. Small substituent changes have great influence on the inhibitory activity (activity cliff). In summary, **6k**, endowed with moderate flexibility, size, and hydrophobicity of R groups, proved to be the most potent NA inhibitor and displayed similar or slightly weaker inhibitory activities than that of OSC towards selected wild-type NAs.

The presence of mutant NA-H274Y has severely limited the clinical applications of OSC and is presently of a great concern<sup>35,36</sup>. Thus, we investigated the inhibitory activity of all compounds against mutant H5N1-H274Y NA. In agreement with our previous data, OSC showed sharply reduced potency (IC<sub>50</sub> = 2.10  $\mu$ M), over 42-fold weaker than that of wild-type H5N1 NA. Among these novel oseltamivir derivatives, **3a-6e** appeared to lack activity against the H5N1-H274Y NA with IC<sub>50</sub> values of over 40  $\mu$ M. It is noteworthy that **6k** and **6i** showed robust activity with IC<sub>50</sub> values of 3.05 and 3.76  $\mu$ M, respectively. Therefore, these compounds could use as lead compounds for further optimisation studies.

#### *In vitro* anti-influenza viral activity

In view of the potent inhibitory activity of several compounds *in vitro*, we further examined their antiviral activity and toxicity in Chicken Embryo Fibroblast cells (CEFs) via cell-based assays that detect the CPE of IAV infection using A/Goose/Guangdong/SH7/2013 (H5N1) and A/Duck/Guangdong/674/2014 (H5N6) strains, consistently with the above enzymatic assays. As previously performed in the enzyme inhibition assays, OSC was selected as a reference compound in parallel. The values of EC<sub>50</sub> (anti-IAV activity) and CC<sub>50</sub> (cytotoxicity) are outlined in Table 2. Notably, none of the tested compounds displayed significant cytotoxicity in CEFs at the highest tested concentration (CC<sub>50</sub> > 200  $\mu$ M).

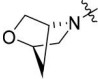
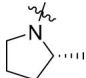
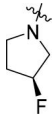
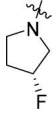
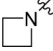

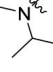
In the case of H5N1 virus, **6g**, **6i** and **6j** showed lower activities (EC<sub>50</sub> = 2.81  $\mu$ M, 2.99  $\mu$ M, and 2.34  $\mu$ M, respectively) compared to OSC (EC<sub>50</sub> = 0.85  $\mu$ M). In contrast, the activity of **6k** (EC<sub>50</sub> = 0.98  $\mu$ M) was comparable to that of OSC, consistently with results obtained in the enzymatic assay. As for the case of H5N6

**Table 1.** Neuraminidase (NA) inhibition of oseltamivir derivatives in chemiluminescence-based assay.

Compds.	R	NA Enzyme-Inhibitory Assay, IC <sub>50</sub> (μM) <sup>a</sup>				
		H1N1 <sup>b</sup> group-1	H3N2 <sup>c</sup> group-2	H5N1 <sup>d</sup> group-1	H5N6 <sup>e</sup> group-2	H5N1-H274Y <sup>f</sup> group-1
3a		4.50 ± 0.69	4.63 ± 0.52	0.85 ± 0.10	0.46 ± 0.061	> 40
3b		4.20 ± 0.11	9.04 ± 0.74	1.17 ± 0.11	0.67 ± 0.10	> 40
3c		12.14 ± 1.10	7.77 ± 0.72	8.25 ± 0.25	5.37 ± 0.062	> 40
3d		4.34 ± 0.36	3.74 ± 0.19	2.63 ± 0.12	1.76 ± 0.040	> 40
3e		8.06 ± 0.48	5.62 ± 0.31	3.80 ± 0.19	2.04 ± 0.15	> 40
6a		3.94 ± 0.11	0.27 ± 0.052	2.08 ± 0.18	1.36 ± 0.11	> 40
6b		0.40 ± 0.033	0.27 ± 0.034	0.39 ± 0.045	0.26 ± 0.015	20.97 ± 0.98
6c		1.40 ± 0.073	0.76 ± 0.024	0.81 ± 0.18	0.57 ± 0.022	> 40
6d		3.10 ± 0.24	1.00 ± 0.11	1.11 ± 0.065	0.59 ± 0.057	> 40
6e		1.99 ± 0.19	0.83 ± 0.034	1.10 ± 0.13	0.75 ± 0.10	> 40
6f		0.43 ± 0.036	0.21 ± 0.019	0.24 ± 0.0078	0.18 ± 0.0099	15.77 ± 0.87
6g		0.19 ± 0.0096	0.16 ± 0.007	0.32 ± 0.015	0.25 ± 0.015	6.69 ± 0.045
6h		0.30 ± 0.0016	0.25 ± 0.013	0.49 ± 0.025	0.50 ± 0.012	6.01 ± 0.24
6i		0.15 ± 0.031	0.16 ± 0.011	0.26 ± 0.015	0.19 ± 0.043	3.76 ± 0.15

(continued)

Table 1. Continued.

Comps.	R	NA Enzyme-Inhibitory Assay, IC <sub>50</sub> (μM) <sup>a</sup>				
		H1N1 <sup>b</sup> group-1	H3N2 <sup>c</sup> group-2	H5N1 <sup>d</sup> group-1	H5N6 <sup>e</sup> group-2	H5N1-H274Y <sup>f</sup> group-1
6j		0.14 ± 0.0064	0.21 ± 0.017	0.59 ± 0.041	0.27 ± 0.0077	11.61 ± 1.56
6k		0.084 ± 0.0072	0.12 ± 0.0063	0.23 ± 0.032	0.15 ± 0.015	3.05 ± 0.47
6l		0.23 ± 0.025	0.40 ± 0.0057	0.69 ± 0.047	0.24 ± 0.018	11.47 ± 1.67
6m		0.37 ± 0.021	0.43 ± 0.031	0.84 ± 0.093	0.18 ± 0.023	14.79 ± 0.21
6n		0.14 ± 0.010	0.21 ± 0.0061	0.42 ± 0.0085	0.18 ± 0.028	11.23 ± 0.59
6o		0.36 ± 0.018	0.56 ± 0.037	0.89 ± 0.072	0.50 ± 0.031	21.74 ± 0.72
6p		0.17 ± 0.0041	0.31 ± 0.0078	0.52 ± 0.080	0.33 ± 0.020	11.88 ± 0.72
OSC	–	0.015 ± 0.00036	0.028 ± 0.0010	0.050 ± 0.0087	0.016 ± 0.0011	2.10 ± 0.26

<sup>a</sup>IC<sub>50</sub>: concentration required to reduce NA activity to 50% of control NA activity Values derive from three experiments and are shown as the mean ± SD.

<sup>b</sup>A/PuertoRico/8/1934.

<sup>c</sup>A/Babol/36/2005.

<sup>d</sup>A/Goose/Guangdong/SH7/2013.

<sup>e</sup>A/Duck/Guangdong/674/2014.

<sup>f</sup>A/Anhui/1/2005.

virus, **6g** and **6i-6k** displayed reduced antiviral activity (EC<sub>50</sub> = 4.06 μM, 5.14 μM, 5.41 μM, and 9.29 μM, respectively). Among them, **6g** exhibited the most potent inhibitory activity, albeit 3-fold weaker than OSC (EC<sub>50</sub> = 1.44 μM), which is not in line with their activities in the enzymatic assay.

Next, we examined compounds' activity against A/PR/8/34 (H1N1) and A/Wisconsin/67/05 (H3N2) strains in MDCK cells by plaque reduction assays (PRA). OSC and ZAN were selected as positive controls for inhibition. The EC<sub>50</sub> and CC<sub>50</sub> (determined via MTT assays) values are summarised in Table 3. No cytotoxicity was observed at the highest tested concentration (250 μM) in MDCK cells.

As for H1N1 strain, all the tested oseltamivir derivatives **6g** and **6i-k** exhibited nearly equivalent potency, with EC<sub>50</sub> values of 0.03 μM, 0.03 μM, 0.03 μM, 0.02 μM, respectively, compared to OSC (EC<sub>50</sub> = 0.02 μM) and ZAN (EC<sub>50</sub> = 0.009 μM). Against H3N2 virus, **6j** showed moderate activity (EC<sub>50</sub> = 0.80 μM), which is 2-fold lower than OSC and 3-fold lower than ZA. Compounds **6g**, **6i**, and **6k** displayed more potent activity against the H3N2 (EC<sub>50</sub> = 0.16 μM, 0.32 μM, and 0.12 μM, respectively) compared to OSC (EC<sub>50</sub> = 0.36 μM). More encouragingly, **6g** and **6k** exerted nearly 2-fold activity enhancement over ZA (EC<sub>50</sub> = 0.27 μM).

### Molecular modeling

In order to gather further insight into the binding mechanisms of novel oseltamivir derivatives in the 150-cavity of NAs, molecular docking

studies of representative compound **6k** bound to the crystal structures of N1 (PDB ID: 3BEQ), N1 (PDB ID: 2HU0), and N2 (PDB ID: 4K1K) were performed by utilising Schrödinger Maestro 12.9 software. The PyMOL 1.3 software was used to visualise the docking results.

As shown in Figure 5(A,B,C), it can be observed that 4-((*r*)-2-methylpyrrolidin-1-yl)benzyl group of compound **6k** was projected towards the 150-cavity of N1 (Figure 5(A,B)) and N2 (Figure 5(C)), while the oseltamivir carboxylic acid part of this compound was well anchored to the active site of NAs, consistent with the binding pattern of OSC. In Figure 5(G), **6k** developed multiple hydrogen bonds with Arg371, Arg292 and Asp151 in the active site (H1N1 NA), in line with OSC binding. Meanwhile, the 4-((*R*)-2-methylpyrrolidin-1-yl)benzyl group extended into the 150-cavity and occupied a hydrophobic pocket consisting of Val116, Thr439, Gly147, Gln136 and Val149. However, compared with OSC, **6k** lost the hydrogen bond between the amide group and Arg152, which may be due to the slight conformational deviation of **6k** caused by the introduction of the amino side chain. Furthermore, the slight conformational deflection made the amide group of **6k** twisting towards Arg156 and established an additional hydrogen bond with it. Although the formation of additional hydrogen bond helped to compensate for the energy loss caused by the destruction of the original hydrogen bond, the distorted conformation might not be optimal for the interaction of NA inhibitors with the active site. This might account for the reduction in the inhibitory activity of **6k**, that was slightly weaker than that of OSC against H1N1 NA.

**Table 2.** Anti-influenza virus activity and cytotoxicity of selected compounds in CEFs.

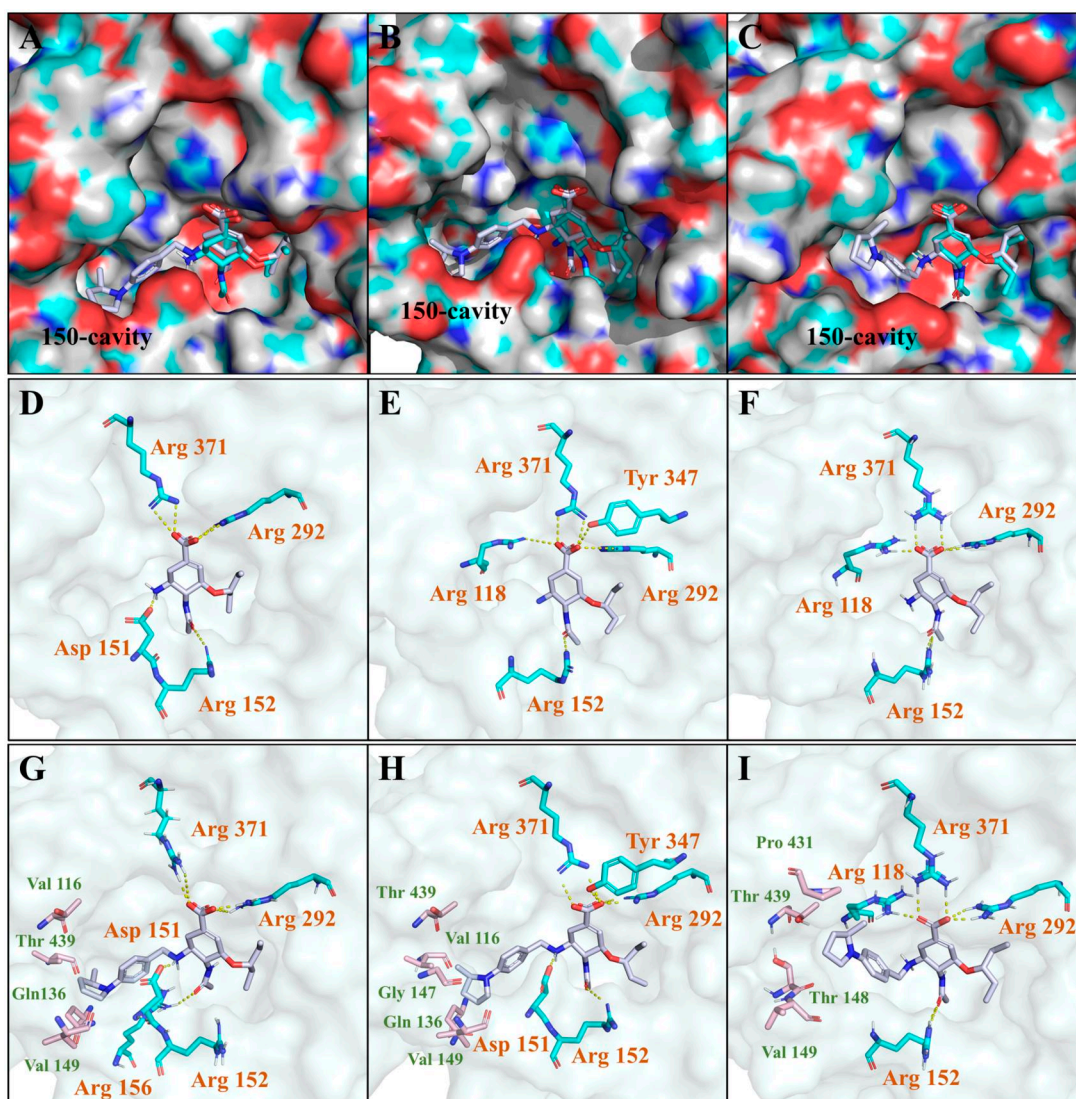
		$EC_{50}^a$ values ( $\mu\text{M}$ ) towards influenza viruses		
Compds.	R	H5N1 <sup>c</sup> group-1	H5N6 <sup>d</sup> group-2	$CC_{50}$ ( $\mu\text{M}$ ) <sup>b</sup>
6g		2.81 ± 0.027	4.06 ± 0.22	>200
6i		2.99 ± 0.44	5.14 ± 0.85	>200
6j		2.34 ± 0.42	5.41 ± 0.51	>200
6k		0.98 ± 0.071	9.29 ± 1.40	>200
OSC	–	0.85 ± 0.16	1.44 ± 0.13	>200

<sup>a</sup> $EC_{50}$ : concentration of compound required to achieve 50% protection of CEF cultures against influenza virus-induced cytopathic effect, presented as the mean ± SD.  
<sup>b</sup> $CC_{50}$ : concentration required to reduce the viability of mock-infected cell cultures by 50%, as determined by the CCK-8 method.  
<sup>c</sup>A/Goose/Guangdong/SH7/2013.  
<sup>d</sup>A/Duck/Guangdong/674/2014.

**Table 3.** Anti-influenza virus activity and cytotoxicity of selected compounds in MDCK cells.

		$EC_{50}^a$ values ( $\mu\text{M}$ ) towards influenza viruses		
Compounds.	R	H1N1 <sup>c</sup>	H3N2 <sup>d</sup>	$CC_{50}$ ( $\mu\text{M}$ ) <sup>b</sup>
<b>group-1</b>	<b>group-2</b>			
6g		0.03 ± 0.03	0.16 ± 0.08	>250
6i		0.03 ± 0.03	0.32 ± 0.08	>250
6j		0.03 ± 0.02	0.80 ± 0.003	>250
6k		0.02 ± 0.01	0.12 ± 0.03	>250
OSC	–	0.02 ± 0.01	0.36 ± 0.16	>250
ZA	–	0.009 ± 0.002	0.27 ± 0.03	>250

<sup>a</sup> $EC_{50}$ : compound concentration that inhibits 50% of virus plaque formation in MDCK cells infected with influenza A viral strains, presented as the mean ± SD and determined by the PRA method.  
<sup>b</sup> $CC_{50}$ : concentration required to reduce the viability of mock-infected cell cultures by 50%, as determined by the MTT method.  
<sup>c</sup>A/PR/8/34.  
<sup>d</sup>A/Wisconsin/67/05.



**Figure 5.** Docking of compound **6k** in the binding site on NA of N1 (PDB ID: 3BEQ), N1 (PDB ID: 2HU0) and N2 (PDB ID: 4K1K). (A, B, C) Superposition of **6k** and OSC with N1 NA and N2 NA, respectively; (D, E, F) The key interactions formed by OSC with N1 and N2 NA, respectively; (G, H, I) The key interactions formed by **6k** with N1 and N2 NA, respectively. Hydrogen bonds are shown as dashed lines (yellow).

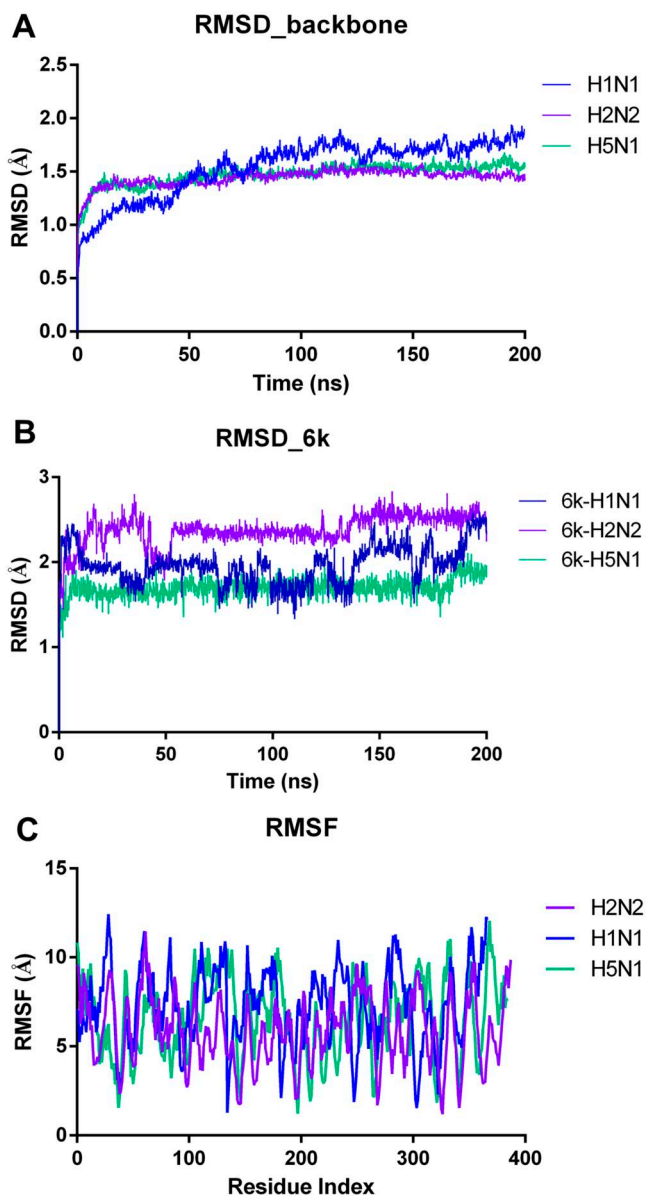
As for H5N1 NA (Figure 5(E,H)), **6k** established similar interactions with OSC at the active site. Multiple hydrogen bonds between carboxylic of **6k** and Arg371, Arg292, Tyr347 and Asp151 were retained as same as OSC. It's a pity that **6k** lost the hydrogen bond with Arg118. The amino group of **6k** formed an additional hydrogen bond with the carbonyl group of Asp151. Compared with the conformation of **6k** binding to H1N1 NA, the 2-methylpyrrolidinyl of **6k** binding to H5N1 NA was positioned outward and also formed wide range of hydrophobic interactions with the amino acid residues that make up 150-cavity.

As shown in Figure 5(F,I), it was suggested that **6k** retained the key interactions of carboxyl group with residues Arg292, Arg371 and Arg118, respectively, which was consistent with the action mode of OSC. Moreover, the conformation of **6k** at the active site was highly overlapped with that of OSC cyclohexene, so that the hydrogen bond between the amide group and Arg152 could still be retained. Although the 150-cavity induced in group-2NA was flatter and shallower, the 4-((R)-2-methylpyrrolidin-1-yl)benzyl group could still stretched into the 150-cavity due to the flexibility of the substituted benzylidene. Compound **6k** might

induce opening of the rigid N2 150-loop and was highly compatible with the active site and 150-cavity. Since **6k** was only incubated with NA for 10 min in the enzyme activity test, it was difficult to induce the completely opening of the rigid N2 150-loop in such a short time. In *in vitro* anti-influenza virus activity assays, **6k** was co-incubated with the H3N2 influenza virus for two days, in which the rigid N2 150-loop could actually be opened by **6k**. This could explain why **6k** had a weaker inhibitory activity against H3N2 NA than OSC in the enzyme activity assay, but it displayed nearly 3-fold activity enhancement over OSC against H3N2 strain in PRA.

#### Molecular dynamics simulations

To further examine the binding stability of **6k** with NA, we performed MD simulation studies of 100 ns initiating from the docked states in Desmond software (Schrödinger Suite version 2022-1). The relevant RMSD (root mean square deviation) and RMSF (root mean square fluctuations) were displayed in Figure 6. The Figure 6(A) illustrates the peaks of the RMSD probability density, indicating the stable conformational variations in the protein structure.



**Figure 6.** The result plots of molecular dynamics simulations. (A) The protein backbone RMSD plot of the NA with **6k** binding throughout the MD trajectory of 200 ns; (B) The ligand heavy atom RMSD plot when bound to the NA; (C) RMSF plot of the protein chain in **6k** bound state.

The ligand heavy atom RMSD analysis in Figure 6(B) revealed the dynamic nature of **6k** binding pose. RMSD values remained quite stable at around 2.0 Å, indicating the strong binding between **6k** and NA. According to the dynamic results, the side chain of **6k** oscillated slightly in the 150-cavity due to its own flexibility. In the RMSF plot (Figure 6(C)), the protein residues fluctuated greatly, further demonstrating that **6k** is tightly bound to NA. These results confirm that the side chain of **6k** can bind closely to the 150-cavity and establish stable interactions with the surrounding residues.

#### *In vitro* neuraminidase inhibitory activity assay of **6k** with different preincubation time with NA

In order to further verify that compound **6k** may induce the opening of N2 150-loop, we carried out neuraminidase inhibitory activity assay of **6k** with different preincubation time with NA. The  $IC_{50}$

data can be seen in Figure 7. As shown in Figure 7(B), preincubation with different time of H3N2 NA with the OSC did not lead to significant changes of the  $IC_{50}$  value (0.023 ~ 0.029  $\mu$ M). However, according to Figure 7(A), the inhibitory activity of **6k** against H3N2 NA was significantly improved with the prolongation of preincubation time. It can be found that longer preincubation time gave lower  $IC_{50}$  values. When the incubation time was 10 min, the  $IC_{50}$  value of **6k** was 0.41  $\mu$ M. When the incubation time was extended to 120 min, the inhibitory activity was greatly improved ( $IC_{50}$  = 0.078  $\mu$ M), being 5.3-fold more potent than **6k** at 10 min incubation time. We also tried to extend the preincubation time to 4 h and 8 h. However, when the enzyme was placed for too long, its activity would be affected, so reliable data were not obtained. Combined with the antiviral activity results of **6k** against H3N2 strain, there is no doubt that **6k** can induce the opening of 150-loop and establish additional interactions, which explained its superior inhibitory activity against H3N2 strain comparable with OSC.

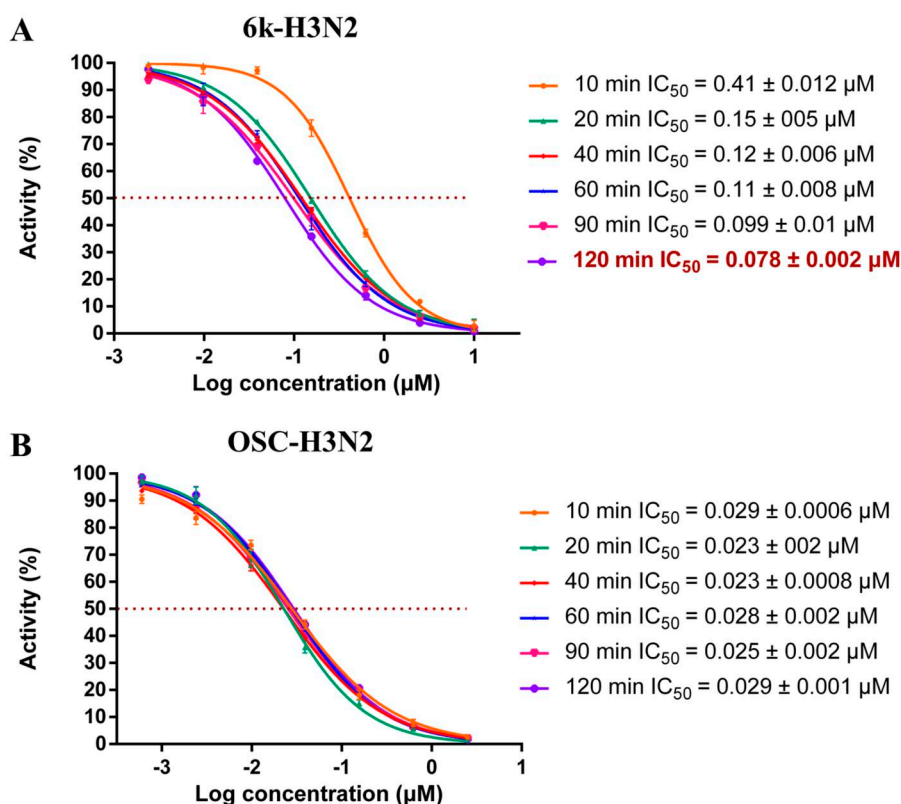
#### *In silico* studies

##### *In silico* prediction of physicochemical properties

As shown in Table 4, all the selected compounds displayed gratifying  $Fsp^3$  values<sup>36</sup>. To further investigate the drug-like properties of representative compounds **6g**, **6i**, **6j**, **6k**, we utilised a free software (<http://www.molinspiration.com/>) to comprehensively address their physicochemical properties. The results confirmed that the parameters of the selected compounds didn't exceed the normal scope and could meet the requirements for Lipinski's "rule of five" concerning MW, nON, nOHNH, nrotb and miLog P. More remarkably, topological polar surface area (TPSA) is an important parameter related to the blood-brain barrier penetration, Caco-2 monolayers permeability and human intestinal absorption of compound. As seen from Table 4, TPSA values of all the compounds were in the range of 9.0 ~ 100.13 Å<sup>2</sup> (<140 Å<sup>2</sup>), confirming their advantages for intestinal absorption (<140 Å<sup>2</sup>) and inability to cross the blood-brain barrier, avoiding detrimental effects on the central nervous system (>60 Å<sup>2</sup>).

#### Conclusion

In summary, based on our previous studies, we designed and synthesized a series of novel N-heterocycles substituted oseltamivir derivatives to explore the chemical space of 150-cavity in NAs. Consistent with our previous findings, the introduction of nitrogen-containing heterocyclic substituents could induce the 150-cavity formation and maintain the inhibitory activity against group-2 NAs. As expected, all the tested novel compounds exhibited potent inhibitory activities against group-1 and group-2 NAs. Among them, compounds **6g**, **6i-6k** displayed moderate inhibitory activities against N1 (H1N1), N2 (H3N2), N1 (H5N1), N6 (H5N6) and mutant N1 (H5N1-H274Y) compared to OSC. Moreover, compounds **6g**, **6i-6k** with low cytotoxicity showed robust anti-IAV potencies against H5N1, H5N6, H1N1, and H3N2 strains in cellular assay. In particular, **6k** exerted the most potent and broad-spectrum anti-IAV activity, with  $EC_{50}$  of 0.98  $\mu$ M, 0.02  $\mu$ M, 0.12  $\mu$ M towards H5N1, H1N1, and H3N2, respectively, which were equivalent or more potent than that of OSC. Additionally, longer preincubation time gave lower  $IC_{50}$  values of **6k**, further proving that N-heterocycles contribute to the opening of the N2 150-loop. The results of docking studies and molecular dynamics simulation studies clearly demonstrated that the side chain of **6k** stably occupies the 150-cavity and the scaffold retains other key interactions



**Figure 7.** The neuraminidase inhibitory activity assay of 6k and OSC with different incubation time with NA. (A) The dose–response–inhibition curve of 6k at different incubation time; (B) The dose–response–inhibition curve of OSC at different incubation time.

**Table 4.** Physicochemical properties of some representative compounds.

Parameter items <sup>a</sup>	6g	6i	6j	6k
Fsp <sup>3</sup> (>0.42)	0.62	0.66	0.58	0.62
MW (<500 Da)	455.60	497.68	471.60	457.62
nON (≤10)	7	7	8	7
nOHNH (≤5)	3	3	3	3
nrotb (≤10)	10	10	10	10
TPSA (<140 Å <sup>2</sup> )	90.90	90.90	100.13	90.90
MV	439.75	490.16	448.74	450.33
miLog p (<5)	3.23	4.29	2.22	3.00

<sup>a</sup>MW: molecular weight; nON: number of hydrogen bond acceptors; nOHNH: number of hydrogen bond donors; nrotb: number of rotatable bonds; TPSA: topological polar surface area;

MV: molar volume; miLog P: molinspiration predicted Log P.

in the active site of NAs. Therefore, compound **6k** deserves to be further studied as a valuable lead compound.

## Acknowledgements

We gratefully acknowledge the financial support from the National Natural Science Foundation of China (NSFC no. 81773574); Science Foundation for Outstanding Young Scholars of Shandong Province (ZR2020JQ31); Foreign cultural and educational experts Project (GXL20200015001); Shandong modern agricultural technology and industry system (SDAIT-21-06); Key Research and Development Program of Shandong Province (2022CXGC010606); China Postdoctoral Science Foundation (2022M711938); Natural Science Foundation of Jiangsu Province (SBK2023041680); Associazione Italiana per la Ricerca sul Cancro, AIRC, grants IG 2016 - ID. 18855 and IG 2021 - ID. 25899 (to A.L.); Ministero dell'Istruzione, dell'Università e della Ricerca, PRIN 2017-

cod. 2017KM79NN (to A.L.); Fondazione Cassa di Risparmio di Padova e Rovigo-Bando Ricerca Covid-2019 No. 55777 2020.0162-ARREST-COV: Antiviral PROTAC-Enhanced Small-molecule Therapeutics against CORONAVIRUSES (to A.L.).

## Author contributions

**Jiwei Zhang and Chuanfeng Liu:** Conceptualisation, Methodology, Formal analysis, Investigation, Resources, Data Curation, Writing - Original Draft, Visualisation

**Ruifang Jia and Jian Zhang:** Supervision, Writing - Review & Editing, Methodology

**Xujie Zhang:** Software

**Chiara Bertagnin, Anna Bonomini, Laura Guizzo:** Resource (Provision of study materials for the *in vitro* anti-influenza virus activity in MDCK cells)

**Yuanmin Jiang, Huinan Jia, Shuzhen Jia:** Resource, Data Curation

**Xiuli Ma:** Resource (Provision of study materials)

**Arianna Loregian:** Resource (Provision of study materials for the *in vitro* anti-influenza virus activity in MDCK cells), Writing - Review & Editing, Supervision, Project administration

**Bing Huang, Peng Zhan, Xinyong Liu:** Writing - Review & Editing, Supervision, Project administration, Funding acquisition

## Disclosure statement

No potential conflict of interest was reported by the authors.



## References

- Tang L, Yan H, Wu W, Chen D, Gao Z, Hou J, Zhang C, Jiang Y. Synthesis and anti-influenza virus effects of novel substituted polycyclic pyridone derivatives modified from baloxavir. *J Med Chem.* 2021;64(19):14465–14476.
- Wang Z, Zalloum WA, Wang W, Jiang X, De Clercq E, Pannecouque C, Kang D, Zhan P, Liu X. Discovery of novel dihydrothiopyrano[4,3-d]pyrimidine derivatives as potent HIV-1 NNRTIs with significantly reduced hERG inhibitory activity and improved resistance profiles. *J Med Chem.* 2021; 64(18):13658–13675.
- Fineberg HV. Pandemic preparedness and response—lessons from the H1N1 influenza of 2009. *N Engl J Med.* 2014; 370(14):1335–1342.
- Swets MC, Russell CD, Harrison EM, Docherty AB, Lone N, Girvan M, Hardwick HE, Visser LG, Openshaw PJM, Groeneveld GH, et al. SARS-CoV-2 co-infection with influenza viruses, respiratory syncytial virus, or adenoviruses. *Lancet.* 2022;399(10334):1463–1464.
- Chen JR, Liu YM, Tseng YC, Ma C. Better influenza vaccines: an industry perspective. *J Biomed Sci.* 2020;27(1):33.
- Shirley M. Baloxavir marboxil: a review in acute uncomplicated influenza. *Drugs.* 2020;80(11):1109–1118.
- Dunn CJ, Goa KL. Zanamivir: a review of its use in influenza. *Drugs.* 1999;58(4):761–784.
- McClellan K, Perry CM. Oseltamivir: a review of its use in influenza. *Drugs.* 2001;61(2):263–283.
- Scott LJ. Peramivir: a review in uncomplicated influenza. *Drugs.* 2018;78(14):1525.
- Kubo S, Tomozawa T, Kakuta M, Tokumitsu A, Yamashita M. Laninamivir prodrug CS-8958, a long-acting neuraminidase inhibitor, shows superior anti-influenza virus activity after a single administration. *Antimicrob Agents Chemother.* 2010; 54(3):1256–1264.
- Loregian A, Mercorelli B, Nannetti G, Compagnin C, Palù G. Antiviral strategies against influenza virus: towards new therapeutic approaches. *Cell Mol Life Sci.* 2014;71(19):3659–3683.
- Baz M, Abed Y, Simon P, Hamelin ME, Boivin G. Effect of the neuraminidase mutation H274Y conferring resistance to oseltamivir on the replicative capacity and virulence of old and recent human influenza A(H1N1) viruses. *J Infect Dis.* 2010;201(5):740–745.
- Kode SS, Pawar SD, Tare DS, Keng SS, Hurt AC, Mullick J. A novel I117T substitution in neuraminidase of highly pathogenic avian influenza H5N1 virus conferring reduced susceptibility to oseltamivir and zanamivir. *Vet Microbiol.* 2019;235: 21–24.
- Wu Y, Wu Y, Tefsen B, Shi Y, Gao GF. Bat-derived influenza-like viruses H17N10 and H18N11. *Trends Microbiol.* 2014; 22(4):183–191.
- Russell RJ, Haire LF, Stevens DJ, Collins PJ, Lin YP, Blackburn GM, Hay AJ, Gamblin SJ, Skehel JJ. The structure of H5N1 avian influenza neuraminidase suggests new opportunities for drug design. *Nature.* 2006;443(7107):45–49.
- Han N, Mu Y. Plasticity of 150-loop in influenza neuraminidase explored by Hamiltonian replica exchange molecular dynamics simulations. *PLoS One.* 2013;8(4):e60995.
- Wu Y, Qin G, Gao F, Liu Y, Vavricka CJ, Qi J, Jiang H, Yu K, Gao GF. Induced opening of influenza virus neuraminidase N2 150-loop suggests an important role in inhibitor binding. *Sci Rep.* 2013;3(1):1551.
- Ju H, Zhang J, Sun Z, Huang Z, Qi W, Huang B, Zhan P, Liu X. Discovery of C-1 modified oseltamivir derivatives as potent influenza neuraminidase inhibitors. *Eur J Med Chem.* 2018;146:220–231.
- Zhang J, Poongavanam V, Kang D, Bertagnin C, Lu H, Kong X, Ju H, Lu X, Gao P, Tian Y, et al. Optimization of N-substituted oseltamivir derivatives as potent inhibitors of group-1 and -2 influenza A neuraminidases, including a drug-resistant variant. *J Med Chem.* 2018;61(14):6379–6397.
- Jia R, Zhang J, Shi F, Bonomini A, Lucca C, Bertagnin C, Zhang J, Liu C, Jia H, Jiang Y, et al. Discovery of N-substituted oseltamivir derivatives as novel neuraminidase inhibitors with improved drug resistance profiles and favorable drug-like properties. *Eur J Med Chem.* 2023;252:115275.
- Zhang J, Murugan NA, Tian Y, Bertagnin C, Fang Z, Kang D, Kong X, Jia H, Sun Z, Jia R, et al. Structure-based optimization of n-substituted oseltamivir derivatives as potent anti-influenza A virus agents with significantly improved potency against oseltamivir-resistant N1-H274Y variant, E. *J Med Chem.* 2018;61(22):9976–9999.
- Jia R, Zhang J, Ju H, Kang D, Fang Z, Liu X, Zhan P. Discovery of novel anti-influenza agents via contemporary medicinal chemistry strategies (2014-2018 update). *Future Med Chem.* 2019;11(5):375–378.
- Jia R, Zhang J, Bertagnin C, Cherukupalli S, Ai W, Ding X, Li Z, Zhang J, Ju H, Ma X, et al. Discovery of highly potent and selective influenza virus neuraminidase inhibitors targeting 150-cavity. *Eur J Med Chem.* 2021;212:113097.
- Jia R, Zhang J, Zhang J, Bertagnin C, Bonomini A, Guizzo L, Gao Z, Ji X, Li Z, Liu C, et al. Discovery of novel boron-containing N-substituted oseltamivir derivatives as anti-influenza A virus agents for overcoming N1-H274Y oseltamivir-resistant. *Molecules.* 2022;27(19):6426.
- Xie Y, Xu D, Huang B, Ma X, Qi W, Shi F, Liu X, Zhang Y, Xu W. Discovery of N-substituted oseltamivir derivatives as potent and selective inhibitors of H5N1 influenza neuraminidase. *J Med Chem.* 2014;57(20):8445–8458.
- Du J, Guo J, Kang D, Li Z, Wang G, Wu J, Zhang Z, Fang H, Hou X, Huang Z, et al. New techniques and strategies in drug discovery. *Chin Chem Lett.* 2020;31(7):1695–1708.
- Muratore G, Mercorelli B, Goracci L, Cruciani G, Digard P, Palù G, Loregian A. Human cytomegalovirus inhibitor AL18 also possesses activity against influenza A and B viruses. *Antimicrob Agents Chemother.* 2012;56(11):6009–6013.
- Nannetti G, Massari S, Mercorelli B, Bertagnin C, Desantis J, Palù G, Tabarrini O, Loregian A. Potent and broad-spectrum cycloheptathiophene-3-carboxamide compounds that target the PA-PB1 interaction of influenza virus RNA polymerase and possess a high barrier to drug resistance. *Antiviral Res.* 2019;165:55–64.
- D'Agostino I, Giacchello I, Nannetti G, Fallacara AL, Deodato D, Musumeci F, Grossi G, Palù G, Cau Y, Trist IM, et al. Synthesis and biological evaluation of a library of hybrid derivatives as inhibitors of influenza virus PA-PB1 interaction. *Eur J Med Chem.* 2018;157:743–758.
- Massari S, Bertagnin C, Pismataro MC, Donnadio A, Nannetti G, Felicetti T, Di Bona S, Nizi MG, Tensi L, Manfroni G, et al. Synthesis and characterization of 1,2,4-triazolo[1,5-a]pyrimidine-2-carboxamide-based compounds targeting the PA-PB1 interface of influenza A virus polymerase. *Eur J Med Chem.* 2021;209:112944.
- Lu C, Wu C, Ghoreishi D, Chen W, Wang L, Damm W, Ross GA, Dahlgren MK, Russell E, Von Bargen CD, et al. OPLS4: improving

- force field accuracy on challenging regimes of chemical space. *J Chem Theory Comput.* 2021;17(7):4291–4300.
32. Sastry GM, Adzhigirey M, Day T, Annabhimoju R, Sherman W. Protein and ligand preparation: parameters, protocols, and influence on virtual screening enrichments. *J Comput Aided Mol Des.* 2013;27(3):221–234.
  33. Sinha SK, Shakya A, Prasad SK, Singh S, Gurav NS, Prasad RS, Gurav SS. An in-silico evaluation of different Saikosaponins for their potency against SARS-CoV-2 using NSP15 and fusion spike glycoprotein as targets. *J Biomol Struct Dyn.* 2021;39(9):3244–3255.
  34. Ju H, Murugan NA, Hou L, Li P, Guizzo L, Zhang Y, Bertagnin C, Kong X, Kang D, Jia R, et al. Identification of C5-NH(2) modified oseltamivir derivatives as novel influenza neuraminidase inhibitors with highly improved antiviral activities and favorable druggability. *J Med Chem.* 2021;64(24):17992–18009.
  35. Bialy D, Shelton H. Functional neuraminidase inhibitor resistance motifs in avian influenza A(H5Nx) viruses. *Antiviral Res.* 2020;182:104886.
  36. Samson M, Pizzorno A, Abed Y, Boivin G. Influenza virus resistance to neuraminidase inhibitors. *Antiviral Res.* 2013; 98(2):174–185.